1. In dozens of places there are grammatical errors, missing punctuation, or improper (or at least less than idea) word usage. I'd encourage the authors to have an English colleague read the paper carefully or to go through an English editing service. It is not in terrible shape, but it could be improved.

Reply:

This paper is further modified for reading.

2. Duan et al. (2017) tackle a similar problem to the present study but in a different approach. I'd encourage the authors to explain why their approach is superior, or at least why it might be preferred in some cases. This could occur in the intro or in the discussion perhaps. In general, the authors should be highlighting that climate change can result in not just differences in the forcing, but also in the system itself (e.g. climate change can alter precipitation regimes which is the hydrologic loading, but it can also alter the hydrologic functioning of a landscape by altering the vegetation and permafrost or seasonally frozen ground distribution)

Duan et al. 2017. Distinguishing streamflow trends caused by changes in climate, forest cover, and permafrost in a large watershed in northeastern China. Hydrol. Process.31

Reply:

Yes! We agree, this is a constructive comment. Accordingly, we discussed the modified method used in this study in Sect 5.2:

Through this modified analysis method, climate change directly impacts (ΔQ_{c1}) are calculated based on existing method, potential climate impacts (ΔQ_{c2}) are analysed by a stepwise linear regression analysis between catchment parameters and potential candidate variables. This method efficiently considered climate change impacts on catchment properties which provide a more reasonable assessment of human activity impacts. With this flexible method all potential factors can be considered in discharge change analysis by stepwise regression analysis, the residual errors of regression analysis possibly indicate impacts of the penitential factors which wasn't directly considered in regression analysis due to record limitation.

Climate changes both impact on system characteristics and system forcing are highlighted in Sect 1 as follow:

Climate changes not only impact on climate forces (precipitation, temperature etc.) but also alter catchment properties (permafrost distribution, vegetation etc.) (Duan et al., 2017).

3. The introduction is generally ok, but I do not like the build up to the objectives at the end. For example, the authors state (P3, L10-13): "these relationships have not been previously examined in the SRYR". So is this just a case study then? If so, perhaps HESS would not be interested in publishing it. I would rather argue that the paper advances the science by further breaking down these offsetting or cumulative discharge disturbances, and specifically examine the role of permafrost degradation –which has been largely ignored in past studies using these statistical approaches.

Reply:

We agree. This sentence is changed into:

Permafrost degradation is mainly caused by climate change therefore it should be considered in climate-induced discharge change analysis in the SRYR.

4. P5, L5, the daily frozen depth of the active layer was identified every month. This makes no sense. How do you identify something with daily frequency on a monthly basis? Also, here the authors say active layer, but is there truly an active layer everywhere – in many places there is no permafrost, correct? Anyway, this is all worded confusingly. The "frozen depth of the active layer" could mean the distance from the land surface to the bottom of the frozen zone (which unless there is a horizontal talik would mean all the way to the bottom of the permafrost during the winter) or it could mean the distance from the land surface to the top of the frozen zone, which would be better called the thawed depth. I'd suggest this be reworded

Reply:

We agree. Thanks for your carefully review. As you said, there is a misleading understand of active layer existed in our manuscript. Permafrost records are not available in these observed records of frozen ground. Because as shown in Figure 2, all the MFD observation stations are located in the transition zone or seasonally frozen ground area. So only MFD can obtained from these stations, but the change of annual maximum frozen depth can also be used to indicate adjacent permafrost change and seasonally frozen ground change in this area. We reworded these sentences in Sect. 2.2:

Monthly mean value was obtained from the daily frozen depth of frozen ground and then used to estimate the annual maximum frozen depth (MFD) of the study period. The MFD value obtained from

5. Figure 3 and P5, L20-25: How were these change points detected? Was any sensitivity analysis conducted on moving these change points incrementally forward or backward in time?

Reply:

These change points are used in a comparison analysis between this study and previous studies. The two change points were carefully chosen in considering change points used in previous studies instead of using theory-based method to detect them.

The two change points (1990, 2002) was first defined by Tang et al. (2013) according to the change of zero-flow frequency. And according to the runoff change pattern as shown in Fig. 2, by using this two change points three periods can be divided: pre-change period (1961-1990), low-flow period (1991-2002), recovery period (2003-2013). The baseline period is same as the climate pre-change period defined by IPCC (IPCC, 2007). The first change points (1990) were also adopted by Zheng et al. (2009) and Meng et al., (2016) to analyse streamflow change in the SRYR. A theory-based detect method was used by Zhao et al. (2009) and three different change points are defined: 1985,1989 and 1989 for JM, MQ and TNH, stations, respectively.

The change points adopted by Zhao et al. (2009) are different from Zheng et al. (2009) and this study, however, by using existing method we obtained similar results of catchment properties change impacts on streamflow change as indicated in Table 4 and P 11 L 29-32.

6. The transition from Eq. 7 to Equations 8-10 was hard for me to follow. This should be reworded

Reply:

The transition is further explained and reworded in P 7 L 21-24 as following:

The sensitivity coefficients f'_P, f'_{E_0} and f'_w in Eq. 7 are defined as partial derivative to respective variables. To eliminate discretization errors, the mean value of the sensitivity coefficients in the pre-change and post-change periods: f^*_P, $f^*_{E_0}$ and f^*_w are defined and used in following study(Jiang et al., 2015):

7. P8, L14-17, a key message of this paper is that climate change can influence the catchment specific parameter. This is likely true, but it should be explained rather than just citing a few other studies. If this is so important, the authors should provide some examples of why this might be from a physical perspective.

Reply:

P8. L14-17 revised as following:

<mark>However, this is not true because catchment relative infiltration capacity and relative soil water storage are also related to climate factors: precipitation intensity and potential evapotranspiration, respectively.</mark>

5 <mark>(Yang et al., 2007;), the catchment specific parameter can also be influenced by climate variability (Donohue et al., 2012), climate type (Williams et al., 2012) and climate change (Jiang et al. 2015).</mark>

8. Related to the above, the paper would be much improved by the authors tying in the physical
10 **hydrologic environment to the statistical analysis results. For example, why would rainfall-runoff processes be altered by changes in permafrost, particularly in the source region of the Yellow River. What soil is there? What slope? Based on this why might the runoff ratios change? Without tying the results to the physical setting, the entire results section comes across as a bit of an arm waving exercise**

15 **Reply:**

Accept, according to this comment, Table 2 is added in the modified manuscript.

Indeed! This article lack of physical explanations due to these analyses are based on statistical method. Potential explanations are added in Sect. 5.2

<mark>However, potential physical explanations can be found in previous studies. It has been found that the</mark>
20 <mark>permafrost degradation could enlarge baseflow in cold regions (Walvoord and Striegl, 2007; Jacques and Sauchyn, 2009; Bense et al., 2012; Evans et al., 2015; Duan et al.,2017). Decrease in MFD because of global warming was considered as a major factor for the increase in baseflow in the Qilian mountain, China (Qin et al. 2016). Additionally, the melt ice within permafrost and increasing hydrologic connectivity fallowing permafrost thaw-induced land-cover change will increase the runoff discharge</mark>
25 <mark>(Connon et al. 2014; Duan et al. 2017). According to these research, further deeper investigations are required to link the rainfall-runoff and base flow behaviors with the physical mechanism of frozen soils and performed in the SRYR.</mark>

30

Minor comments

I'd invite the authors to refer to Wang et al. 2018, which has some overlap with the present study (especially geographically) along themes related to changing MFD. They may be able to feed some data from this prior paper into their statistical approach.

5

Wang et al. 2018. Historical and future changes of frozen ground in the upper Yellow River Basin. Global and Planetary Change, 172, 199-2011

Accept! Cited in Sect 1, There is about 23% of the permafrost in the SRYR degraded to seasonally
10   frozen ground during the past 5 decades (Wang et al., 2018).

P1, L29 'are facing serious water shortages' – use of the present tense here might warrant a more recent citation as Yang et al. (2004) is now 14 years old.

Reply:

15   Modified as follow:

Due to the dry climate and heavy water demands, people in the Yellow River basin are facing serious water shortages in 1990s.

P3, L7-8, 'permafrost thawing to surface water discharge' - I don't really like this wording.
20   **It seems to imply that permafrost thaw produces streamflow (i.e. the meltwater is a significant contributor to streamflow). If so, that would surely be an incredibly fast thaw rate!**

Reply:

Accept. Modified as follow：

25   Permafrost degradation will increase the depth and length of subsurface flow paths and the lag-times of subsurface water flow from infiltration to surface water discharge.

P3, L30-40, I find this description confusing. The opposite ends of the permafrost

spectrum are continuous and isolated, so why would the authors lump those into a

single 'continuous' category. Also Figure 1 shows alpine permafrost, but does not

indicate if this is continuous or discontinuous. I guess that is what the authors are

explaining in that paragraph – the classification system is not standard

5   **Reply:**

Accept! The classification of permafrost was further explained in Sect. 2.1 P4 L1- 7.

For this map, there are three permafrost classifications: predominantly continuous permafrost (70-80%), isolated permafrost (40-60%) and alpine permafrost. This classification scheme is different from that of the International Permafrost Association (IPA) (Cheng and Wu, 2007; Ren et al., 2012). In Figure 1b,

10   the predominantly continuous permafrost and the isolated permafrost are further combined into the plateau permafrost in the Tibetan Plateau (Ren et al., 2012).

Figure 1 was further modified according to this comment and attached in this reply.

P4, L3, Why is the SRYR unique? This is not explained

Reply:

15   It is explained in P4 L 6-7. Due to the water resource significance and unique landscape, the SRYR provides an ideal location to observe the hydrological effects of degrading permafrost with climate change.

P17, L15, what about aerial geophysical methods in permafrost? See Minsley et al.

Minsley et al. 2012, Airborne electromagnetic imaging of discontinuous permafrost.

20   **Geophys. Res. Lett.**

Reply:

Yes! Indeed! Airborne electromagnetic method is different from those classical methods. This kind of method can be employed in a larger area catchment. However, long-term dynamic state of permafrost is difficult to be obtained by this kind of method.

25

P17, L18-24, this paragraph is worded as though it were a key springboard to future

work. I found the logic in the section hard to follow. Perhaps the wrong word is used

in some sentence, or perhaps my mind is dense after another long day. But they seem

to suggest that decreasing MFD is a positive factor and that this is enigmatic – but

30   **then they indicate later that Qin et al. 2016 showed this. Are they saying there are no**

physical explanation for this or that it is unusual?

Reply:

Qin et al. 2016 did show that positive correlation between decreased MFD and increased baseflow. However, it just emphasises permafrost degradation impacts on groundwater discharge are different from total discharge analysed in this study. Potential physical explanations were added in Section 5.2 as mentioned in reply of comments 8.

Climate-induced hydrologic change in the source region of the Yellow River: a new assessment including varying permafrost

Pan Wu[1], Sihai Liang[1], Xu-Sheng Wang[1], Yuqing Feng[1], Jeffrey M. McKenzie

[1]School of Water Resources and Environment, China University of Geosciences (Beijing), Beijing, 100083, P. R. China.

[2]Earth and Planetary Sciences, McGill University, Montreal, Quebec, H3A 0E8

Correspondence to: Sihai Liang (liangsh@cugb.edu.cn)

Abstract. The source region of the Yellow River (SRYR) provides 35% of the rivers annual discharge but is very sensitive to the climate change. The change in discharge from the SRYR has been attributed to both climatic and anthropogenic forces, and previous estimates of the impact of human activities on the change in discharge have been higher than 50% of the total change. Considering the very low population density and limited land use change, this result is potentially inconsistent. Our study modifies the traditional Budyko separating approach to identify and quantify the climatic causes in discharge changes. Application of this new approach to the SRYR now highlights the role of the degrading permafrost, based on long-term observation data of the maximum frozen depth (MFD). Our results show that over the past half-century, the change in discharge in the SRYR was primarily controlled by climate change rather than local human activities. Increasing air temperature is generally a negative force on discharge whereas it also causes permafrost to degrade - a positive factor on discharge generation. Such conflicting effects enhance the uncertainty in assessments of the hydrological response to climate change in the SRYR.

1. Introduction

In the past five decades, climate has changed dramatically at the global scale (IPCC，2007), resulting in long-term impacts on global river systems (Abdul Aziz and Burn, 2006; Birsan et al., 2005; Chen et al., 2014; Chiew et al., 2009). The response of hydrological basins in the Tibetan Plateau due to climate change is a major concern for the management of water resources, particularly in China. The water balance of headwater basins in the Tibetan Plateau is influenced by climate change at different levels

7

(Immerzeel et al., 2010; Liang et al., 2013; Su et al., 2016). Originating from the Tibetan Plateau, the Yellow River is the second longest river in China. The river's streamflow intensity has undergone large changes in the past 50 years, primarily observed by a sharp decreased in many sub-basins during the 1990s (Liu and Zheng, 2004) . Due to the dry climate and heavy water demands, people in the Yellow

5   River basin are facing serious water shortages in 1990s (Yang et al., 2004).

The source region of the Yellow River (SRYR) is a large basin above the Tangnaihai hydrological station (Figure 1) which contributes about 35% of the total annual streamflow, but has an area that is only 16% of the total Yellow River basin (Lan et al., 2010). In the 1990s, streamflow from the SRYR

10   significantly decreased with increasing cases of flow cutoff (Yang et al., 2004; Zhang et al., 2008; Zheng et al., 2007). As shown in Table 1, the causes of the decreased flow within the SRYR and other sub-basins of the Yellow River have been extensively investigated in the literature. However, there are disagreements as to the causes of the observed decreases in streamflow. Many researchers suggested that climate change (manifested as decreased precipitation and increased evapotranspiration) is the

15   primary cause of the decrease in streamflow (Cuo et al., 2013; Liang et al., 2010; Meng et al., 2016; Tang et al., 2013). Other researches proposed that the decrease in discharge was mainly caused by changes in catchment properties (Zheng et al., 2009, Zhao et al., 2009). For example, Zheng (2009) found that the decrease in streamflow in the 1990s was a result of climate change and land use change but highlighted that the land use change was more important and that it contributed to about 70% of the

20   total change in streamflow. Zhao (2009) suggested that 65% of the streamflow change in the upper catchment of the Jimai hydrological station could be attributed to the effects of human activities. This conclusion is potentially at odds with the very low population density in the area above the Tangnaihai hydrological station (about 6 people/km^2, 2003 census data) and in the area above the Huangheyan station (0.34 people/km^2) (Liang et al., 2010). From 1990 to 2000, the change in land use in the SRYR

25   was generally less than 5%, though a few sites exhibited 5-15% of the change (Wang et al., 2010). Therefore, it is not easy to attribute the negligible impact of human activities and land use changes to more than 50% of the change in the discharge of the SRYR.

One reason for the divergent (and potentially problematic) findings from previous analysis on the

30   climate elasticity of the streamflow in the SRYR (Zheng et al., 2009, Zhao et al., 2009) may be the misattribution of the change in catchment properties. The concept of climate elasticity of discharge was widely used to separate the change in streamflow into different components, including climate changes, landcover changes and human activities that induced by changes in climatic forces and catchment properties (Arora, 2002; Fu et al., 2007; Zheng et al., 2009; Yang and Yang; 2011). The sensitivity

35   method (Roderick and Farquhar, 2011) and decomposition method (Wang and Hejazi 2011) were also developed with the process like the climate elasticity analysis method. Previously the effect of change in catchment properties was usually attributed to human activities or land use change (Ma et al., 2008, Zheng et al., 2009, Zhao et al., 2009). This attribution would lead to a bias in the findings because the

catchment properties could also depend on the climate condition (Yang et al., 2007; Williams et al., 2012; Donohue et al., 2012; Jiang et al. 2015). Thus, the change in catchment properties in the SRYR should be re-examined.

5 The other poorly known factor in the SRYR is the hydrological impacts of the changes in the permafrost distribution. Permafrost is defined as a subsurface region in which the temperature is below 0 °C for 2 or more consecutive years. The SRYR is widely underlain by permafrost, particularly in the area above the Jimai station (Figure 1; Zhou et al., 2000) where the altitude is relatively high. In the recent 50 years, the air temperature in the SRYR increased at an average rate between 0.31°C /10a and
10 0.35°C /10a (Cuo et al., 2013; Hu et al., 2011). Due to this warming trend, permafrost has warmed and degrading, and the depth of the annual active layer has increased in the upper catchment above Jimai station (Luo et al., 2014a; Luo et al., 2014b). There is about 23% of the permafrost in the SRYR degraded to seasonally frozen ground during the past 5 decades (Wang et al., 2018). Climate changes not only impact on climate forces (precipitation, temperature etc.) but also alter catchment properties
15 (permafrost distribution, vegetation) (Duan et al., 2017). Permafrost degradation will increase the depth and length of subsurface flow paths and the lag-times of subsurface water flow from infiltration to surface water discharge (Frampton et al., 2011, Kurylyk et al., 2014). Degrading permafrost could also accelerate the flow recession process and increase local hydrological circulation (Lyon and Destouni, 2010; Lyon et al., 2009; Cuo et al., 2015), change aquifer permeability, and increased base flow
20 (Walvoord and Striegl, 2007; Bense et al., 2012; Evans et al. 2015). Permafrost degradation is mainly caused by climate change therefore it should be considered in climate-induced discharge change analysis in the SRYR.

The objective of this study is to develop a new assessment of the causes of discharge changes in
25 different sub-basins of the SRYR. A specific catchment parameter, based on the Budyko framework, is applied to represent the properties of the drainage basins. Correlation analysis with multiple models is performed to reveal the relationships between the time-varying catchment parameter and potential drivers of hydrologic change, such as the climatic forcing and permafrost degradation.

2 Study area and data processing

30 ### 2.1 Catchments and sub-basins

The Yellow River originates from the Tibetan plateau, flows across northern China from west to east, and eventually empties into the Bohai Sea. The source region of the Yellow River (SRYR) is in the northeastern Tibetan Plateau where there is extensive permafrost (Figure 1). The Tangnaihai hydrological station is at the outlet of the SRYR, and receives the discharge from more than 120000
35 km^2 catchment area. The SRYR contributes about 35% of the total annual river flow (Lan et al., 2010) so that it is an essential site for the Chinese water resources. Two major lakes, Gyaring and Ngoring,

are located within the highest sub-basin controlled by the Jimai hydrological station. Another hydrological station, Maqu, monitors the middle reaches between Jimai and Tangnaihai.

The landscape of the study area is characterized by permafrost that has undergone significant degradation since the 1980s (Jin et al., 2010). The distribution of the permafrost in the 1980s is reported in the Map of Snow, Ice, and Frozen Ground in China (1988) published by the Environmental and Ecological Science Data Center for West China, National Natural Science Foundation of China (http://westdc.westgis.ac.cn). For this map, there are three permafrost classifications: predominantly continuous permafrost (70-80%), isolated permafrost (40-60%) and alpine permafrost. This classification scheme is different from that of the International Permafrost Association (IPA) (Cheng and Wu, 2007; Ren et al., 2012). In Figure 1b, the predominantly continuous permafrost and the isolated permafrost are further combined into the plateau permafrost in the Tibetan Plateau (Ren et al., 2012). Due to the water resource significance and unique landscape, the SRYR provides an ideal location to observe the hydrological effects of degrading permafrost with climate change.

In this study, the SRYR area is divided into three sub-basins from the headwaters to the SRYR outflow: the Jimai (JM) basin, the Jimai-Maqu (MQ) basin, and the Maqu-Tangnaihai (TNH) basin. Historical observation data are collected and re-organized for the three sub-basins. A significant difference between the sub-basins is the coverage area of the permafrost. As shown in Figure 1b, almost all the JM (80%) is covered by the continuous permafrost whereas in the MQ only 23% of the basin area has is occupied by the continuous permafrost and alpine permafrost. In the TNH, 46% of the basin area is occupied by the permafrost (Table 2).

2.2 Data processing

Annual discharge data since 1961 at the Jimai, Maqu, Tangnaihai stations were obtained from the Yellow River Conservancy Commission (YRCC) and Loess Plateau Data Center (http://loess.geodata.cn). Daily meteorological data between 1961 and 2013 at 18 meteorological stations (Figure 1b) within the SRYR or in the surrounding areas were collected from the China Meteorological Administration (CMA), including precipitation, air temperature, wind speed at 10 m height, relative humidity and sunshine duration. The potential evapotranspiration was calculated with the FAO Penman-Monteith equation (Allen et al., 1998). These data were applied to derive the annual precipitation (P, mm), annual precipitation intensity (I, mm/d), annual mean temperature (T, °C) and annual potential evapotranspiration (E_0, mm) from 1961 to 2013 at the meteorological stations.

The annual precipitation intensity, I, was calculated at the meteorological stations, and defined as the sum of daily precipitation divide by the number of days with rainfall for every year. Then, gridded data of P, E_0, T and I were created using the inverse distance weighted technique (IDW), with the resolution

of $0.01° \times 0.01°$. Based on the gridded data, the mean values of P, E_0, T and I in the three sub-basins were calculated for each year from 1961-2013.

We do not correct the meteorological data for elevation effects because the properties of the elevation effects are poorly known in the SRYR. However, it is expected that the elevation-dependent distributions of these factors are mostly included within the IDW results. In general, the elevation of ground surface in the study area increases gradually from the east to the west and creates a climate gradient parallel to the altitude gradient that is exhibited in the differences in the observed meteorological data (Figure 1b). For the annual precipitation, we found that these IDW data at the catchment scale agreed with TRMM data (Tropical Rainfall Measurement Mission) 3B42 data (Tong et al., 2014) which show a great performance in streamflow simulation in upper Yellow and Yangtze River basins on the Tibetan Plateau (Hao et al., 2014). The IDW interpolation is adopted in this study to fully capture the collected P, E_0, T and I data at the weather stations.

Daily observations of frozen ground at 11 meteorological stations (Figure 1b) was collected by CMA. Monthly mean value was obtained from the daily frozen depth of frozen ground and then used to estimate annual maximum frozen depth (MFD) of the study period. The MFD value obtained from the monthly mean frozen depth was used to indicate the degradation of adjacent permafrost and seasonally frozen ground. Typical variation patterns of the mean frozen depth are shown in Figure 2. The mean frozen depth exhibits a decreasing trend at most of the observation sites, especially in the period after 1980. The MFD data of the observation stations in and around each sub-basin show the same tend (Figure 2). In considering of the different record lengths of MFD in different observation stations, a station with the longest record is selected to account for the representative MFD data in each sub-basin. Therefore, M5, M10, and M14 are selected for JM, MQ and TNH, respectively, as that shown in Figure 1b. The station M14 is not located in the MQ sub-basin but it exhibits the same variation trend of MFD with that observed at stations in the MQ basin (M12, M13 and M16) with shorter records. However, M17 shows little variation compared to the other sites because it is located at alpine permafrost and therefore is not used in this study.

Figure 3 shows that discharge change can be divided into three periods: pre-change period from 1961-1990, low-flow period from 1991-2002 and recent period from 2003-2013. The two change points (1990, 2002) was first defined by Tang et al. (2013) according to the change of zero-flow frequency. The baseline period is same as the climate pre-change period defined by IPCC (IPCC, 2007).

3 Methods

To assess the impact of degrading permafrost on the hydrology of the sub-basins, we use a new analysis approach compared to previous studies from the SRYR. First, the Budyko framework is

applied to investigate the shift of mean annual water balance. Second, the change in the discharge is directly partitioned into two components: climatic-induced (ΔQ_c) and catchment properties change induced (ΔQ_w), using three existing methods in previous studies based on the Budyko framework. A modified method is introduced using a covariate analysis to further partition the catchment properties

5   change induced changes in discharge into two components: correlation with changes in $P(I)$, E_0 and T, and unknow forcing. Finally, the relationship between the unknow forcing change in the discharge and the degrading permafrost was investigated.

3.1 Budyko framework

10   Evapotranspiration in a catchment can be calculated from the water balance equation as follow:

$$E = P - Q - \Delta S \tag{1}$$

where the annual evapotranspiration, E, the annual precipitation, P, and the annual discharge, Q, are calculated as the average flux to and from the basin, whereas ΔS is the change of storage during an accounting period. In a long period (usually more than 10 years), the change in storage (ΔS) is

15   negligible for the mean annual water balance so that $E=P-Q$ can be applied.

Budyko (1974) demonstrated that the mean annual evapotranspiration ratio (E/P) is mainly controlled by the mean aridity index (= E_0/P where E_0 is the annual potential evapotranspiration). This hypothesis is the underlying principle of the Budyko framework in building a straightforward estimation formula

20   for E/P versus E_0/P. Non-parametric and one-parameter formulas have been proposed in the literature (Table 3). Non-parametric formulas were proposed before 1980 to represent a deterministic regression curve for the relationship between E/P and E_0/P from a global dataset. One-parameter formulas were developed after 1980 to introduce catchment specific parameters (w, n and α in Table 3) so that a group of regression curves for the relationship between E/P and E_0/P were formed for different types of

25   catchments. The one-parameter formulas were more practical in comparison to the non-parametric formulas where the specific catchment parameter can represent the variable catchment properties (Xiong and Guo, 2012). Accordingly, the long-term mean evapotranspiration ratio can be calculated as follows:

$$\frac{E}{P} = F\left(\frac{E_0}{P}, \ w\right) \tag{2}$$

30   where w is the specific catchment parameter, $F()$ denotes an empirical formula. The long-term mean discharge Q can then be calculated as:

$$Q = P - E = P\left(1 - F\left(\frac{E_0}{P}, w\right)\right) = f(P, E_0, w) \tag{3}$$

here f () is the function derived from $F()$. The parameter, w, can be inversely determined with observation data of Q, E_0, and P, for a long period using the mean annual water balance, or for year-by-year patterns using a moving average method (Jiang et al., 2015).

3.2 Existing separating methods for climatic and anthropic causes of the change in discharge

In general, the change in discharge (ΔQ) is attributed to the impacts of both climate change and human activities. Equation (3) shows the general response of discharge on the climate so that it can indicate the natural climatic change in discharge (ΔQ_c). Thus, the difference between the actual change (ΔQ) and the climatic change (ΔQ_c) can be attributed to the anthropic cause, which herein is denoted as ΔQ_h. Three existing methods have been developed in the literature to partition ΔQ into ΔQ_c and ΔQ_h, using different definitions. However, as compared by Wang and Hejazi (2011), these separation methods obtain similar results when they were applied for the same catchments.

3.2.1 Climate elasticity method

The concept of climate elasticity was proposed by Schaake (1990) for one variable (Precipitation). This method has been subsequently modified to considering two variables, precipitation and evaporation (Arora, 2002; Dooge et al., 1999; Kuhnel et al., 1991), and is described as:

$$\Delta Q_c = \frac{\partial f}{\partial P}\Delta P + \frac{\partial f}{\partial E_0}\Delta E_0 = f'_P \Delta P + f'_{E_0} \Delta E_0 \qquad (4)$$

where f'_P and f'_{E_0} are the partial derivatives of $f()$ in Eq. (3) by treating the catchment specific parameter (w) as a constant. The w value must be determined for a period in the natural state and then regarded as a constant. The anthropic change (ΔQ_h) can then be obtained by:

$$\Delta Q_h = \Delta Q - \Delta Q_c \qquad (5)$$

3.2.2 Sensitivity method

The sensitivity method differs from the climate elasticity method as the catchment specific parameters are variable (Roderick and Farquhar, 2011):

$$\frac{dQ}{Q} = \left[\frac{P}{Q} f'_P\right]\frac{dP}{P} + \left[\frac{E_0}{Q} f'_{E_0}\right]\frac{dE_0}{E_0} + \left[\frac{w}{Q} f'_w\right]\frac{dw}{w} \qquad (6)$$

where the terms in the square brackets are called the sensitivity coefficients, f'_P, f'_{E_0} and f'_w, and they directly represent the sensitivities of the discharge with respect to the changes in P, E_0 and w, respectively. Accordingly, the change in discharge can be estimated as:

$$\Delta Q = f'_P \Delta P + f'_{E_0} \Delta E_0 + f'_w \Delta w \qquad (7)$$

The sensitivity coefficients f'_P, f'_{E_0} and f'_w in Eq. 7 are defined as partial derivative to respective variables (P, E_0 and w). To eliminate discretization errors, the mean value of the sensitivity coefficients

13

in the pre-change and post-change periods: f_P^*, $f_{E_0}^*$ and f_w^* are defined and used in following study(Jiang et al., 2015):

$$f_P^* = \frac{1}{2}\left[f_P'(P,E_0,w) + f_P'(P+\Delta P, E_0 + \Delta E_0, w + \Delta w) \right] \tag{8}$$

$$f_{E_0}^* = \frac{1}{2}\left[f_{E_0}'(P,E_0,w) + f_{E_0}'(P+\Delta P, E_0 + \Delta E_0, w + \Delta w) \right] \tag{9}$$

5
$$f_w^* = \frac{1}{2}\left[f_w'(P,E_0,w) + f_w'(P+\Delta P, E_0 + \Delta E_0, w + \Delta w) \right] \tag{10}$$

The climatic and anthropic changes in discharge are considered as

$$\Delta Q_c = f_P^* \Delta P + f_{E_0}^* \Delta E_0 , \ \Delta Q_h = \Delta Q_w = f_w^* \Delta w \tag{11}$$

where ΔQ_w is applied in this study to denote the change in discharge induced by the change in the specific catchment parameter. This method estimates the variable w values and assumes that Δw is

10 caused by the human activities such as the change in land use.

3.2.3 Decomposition method

For the decomposition method (Wang and Hejazi, 2011), different parts of the change in discharge are estimated from:

15
$$\Delta Q_c = f(P+\Delta P, E_0 + \Delta E_0, w) - f(P,E_0,w) \tag{12}$$

$$\Delta Q_h = f(P,E_0,w+\Delta w) - f(P,E_0,w) = \Delta Q - \Delta Q_c \tag{13}$$

From Eq. 13 we see that this method also attributes Δw to human activities.

3.3 Identifying the climatic impact on the catchment specific parameter

20 In the existing approaches, the change in the catchment specific parameter and the induced change in the discharge are attributed to human activities, *e.g.*, change in land use. However, this is not true because catchment relative infiltration capacity and relative soil water storage are also related to climate factors: precipitation intensity and potential evapotranspiration, respectively (Yang et al., 2007;), the catchment specific parameter can also be influenced by climate variability (Donohue et al.,

25 2012), climate type (Williams et al., 2012) and climate change(Jiang et al. 2015). Thus, it is necessary to further separate Δw into climatic change, Δw_c, and anthropic change, Δw_h, as:

$$\Delta w = \Delta w_c + \Delta w_h \tag{14}$$

where Δw_c is accounts for estimating the climatic change in the discharge.

14

It is difficult to directly separate Δw_c and Δw_h from the w values year-by-year during a given period because the relationship between w and the catchment conditions is not well known in the literature. In this study, we apply an indirect method which is similar to the approach in Jiang et al. (2015). The w value is assumed to be linearly correlated with some explanatory variables as follow

$$w = \beta_0 + \beta_1 \frac{Pre}{Pre_m} + \beta_2 \frac{E_0}{E_m} + \beta_3 \frac{T}{T_m} + X \qquad (15)$$

where β_0, β_1, β_2 and β_3 are coefficients, T is the annual mean air temperature, Pre represents the characteristics of precipitation (two forms was considered: precipitation, P, or precipitation intensity, I) and E_0 is the annual potential evapotranspiration.

Each of the variables is normalized by the absolute mean annual value, indicated by subscript m (Pre_m, E_m and T_m). T_m values are 1.48°C, 1.35°C and 1.27°C for JM, MQ and TNH, respectively. The annual precipitation intensity was extracted for the sub-basins in data-processing (Sect. 2.2). Due to the very low population density (2003 census data; Liang et al., 2010) and a slight land use change (Wang et al., 2010) in the SRYR, human activities were not directly considered in this study. Thus, X is taken as a residual error from the linear regression with β_0, β_1, β_2 and β_3.

Similar to using Eq. (15), Jiang et al. (2015) proposed a general linear function to represent the dependency of w on a number of possible explanatory variables and determined the β_i (i=0, 1, 2…) values through the covariate analysis and the Akaike's information criterion (AIC) for multiple models. Three functional forms (i.e., identity, exponential, and logarithmic) may be used for each variable, however, only the identity form was used in this study for simplification. The β_i (i=0, 1, 2…) values were determined through stepwise regression analysis. In each step of stepwise regression analysis, a variable is considered for addition to, or subtraction from, the set of explanatory variables based on a sequence of F-tests, and the variance inflation factor (VIF) was used to diagnose the collinearity. The selected model has the highest R-squared value and contains variables with VIF< 10. A high VIF value indicates the presence of multicollinearity, a VIF value of 10 is often adopted to diagnose the multicollinearity. In practice, VIF < 10 indicates ignorable multicollinearity among these variables (Neter et al., 1989; Hair et al., 1995; Jolliffe, 2002; Jou and Cho, 2014).

According to Eq. (15), the climatic change in the specific catchment parameter, Δw_c, can be estimated as

$$\Delta w_c = \beta_1 \Delta \overline{Pre} + \beta_2 \Delta \overline{E}_0 + \beta_3 \Delta \overline{T} \qquad (16)$$

15

where $\overline{Pre}$ ($=P/P_m$ or I/I_m), $\overline{E}_0$ ($=E_0/E_m$) and $\overline{T}$ ($=T/T_m$) are the normalized value of P (or I), E_0 and T, respectively. However, Eq. (16) misses the impact of the change in permafrost and would be not sufficient to represent all climatic forces on the catchment parameter in the study area. Thus, a modified formula is proposed in this study to check the impact of permafrost change:

5

$$\Delta w_c = \beta_1 \Delta \overline{Pre} + \beta_2 \Delta \overline{E}_0 + \beta_3 \Delta \overline{T} + \beta_4 \Delta \overline{D} \tag{17}$$

where $\overline{D}$ and β_4 are the normalized MFD used to indicate the status of the permafrost and the relevant coefficient, respectively. The term $\beta_4 \overline{D}$ should be included in X in Eq. (15) and can be identified from the correlation between X and $\overline{D}$.

10   In a different way from the existing decomposition methods, we define:

$$\Delta Q_w = f(P, E_0, w + \Delta w) - f(P, E_0, w) \tag{18}$$

$$\Delta Q_{c1} = f(P + \Delta P, E + \Delta E_0, w) - f(P, E_0, w) \tag{19}$$

$$\Delta Q_{c2} = \frac{\Delta w_c}{\Delta w} \Delta Q_w \tag{20}$$

and take the climatic change in discharge as the summation of ΔQ_{c1} and ΔQ_{c2}:

15

$$\Delta Q_c = \Delta Q_{c1} + \Delta Q_{c2} \tag{21}$$

where ΔQ_{c1} equals to ΔQ_c in Eq. (13), which depends on the changes in P and E_0; and ΔQ_{c2} is the additional climatic change in the discharge induced by Δw_c. The anthropic change in discharge can then be estimated as $\Delta Q_h = \Delta Q - \Delta Q_c$. The comparison between results of Eq. (16) and Eq. (17) indicates the impacts of the permafrost degradation on runoff in the SRYR, as presented in Sect. 4.2 and 4.3.

20   **3.4 Selection of the Budyko formula**

Among the one-parameter formulas (Table 3), the Fu's equation (Fu, 1981; Zhang et al., 2004) yields the first analytical solution of the Budyko hypothesis. The equation proposed by Zhang et al. (2001) is an empirical solution which does not agree with the wet boundary condition when $w=2$ (Yang et al., 2008). Yang et al. (2008) presented a new analytical derivation of Choudhury's (1999) solution and
25   obtained a very high ($R^2=0.999$) linear correlation between the catchment specific parameter in the Fu's equation and that in the Choudhury's equation. Similar results were obtained by other researches based on Fu's equation and Choudhury's equation (Yang et al., 2008, Wang and Hejazi, 2011, Jiang et al., 2015). To avoid repetition, only the Fu's equation is applied in this study.

30   Substituting the Fu's equation into Eq. (3), we get:

$$Q = f\left(P, E_0, w\right) = \left(P^w + E_0{}^w\right)^{\frac{1}{w}} - E_0 \tag{22}$$

Accordingly, f_P', f_{E_0}' and f_w' are given by:

$$f_P' = P^{w-1}\left(P^w + E_0{}^w\right)^{\frac{1-w}{w}} \tag{23}$$

$$f_{E_0}' = E_0{}^{w-1}\left(P^w + E_0{}^w\right)^{\frac{1-w}{w}} - 1 \tag{24}$$

5

$$f_w' = \frac{\left(P^w + E_0{}^w\right)^{\frac{1}{w}}}{w}\left[\frac{P^w lnP + E_0{}^w lnE_0}{P^w + E_0{}^w} - \frac{\ln\left(P^w + E_0{}^w\right)}{w}\right] \tag{25}$$

To inversely obtain the w value from observation data, we simply use $E=P-Q$ but include an uncertainty of the impact of the ignored change in water storage. To minimize the effect of change in storage, the moving average method, with a sufficient width of the moving window, is applied (Jiang et al., 2015). A moving window of 11 years was adopted by Jiang et al. (2015). In this study, the effective

10   width of the moving window for the basins in the SRYR of 7, 9, 11, 15 and 19 years were tentatively considered in our analysis.

4. Results and comparisons

4.1 Results of the existing separating methods

As described in Sect. 2.2, the study period between 1961 and 2013 is divided into three typical sub-

15   periods. The period of 1961-1990 is a reference to account for the change. For period 1991-2002, P decreased (3% - 12.4%) and E_0 slightly increased (0%-3.3%) with time in the whole area. In the 21st Century (2003-2013), P increased (1%-15.5%) across the whole study area with a sharp increase (more than 5.7%) in the JM and TNH sub-basins. ΔE_0 varied from -2.1% to 7.4% in the 21st century.

20   Using the period of 1961-1990 as the reference period, the change in discharge was partitioned with three existing methods (climate elasticity method, sensitivity method, and decomposition method) for the three sub-basins in the two periods, 1991-2002 and 2003-2013 (Table 4). The catchment specific parameter for the climate elasticity method, $w=2$, is applied according to Zheng et al. (2009). For the sensitivity method and decomposition method, w is inversely calculated from Fu's equation according

25   to the mean water balance in different periods. All the estimated changes in discharge are expressed in Table 4 as the percentage of the mean annual discharge during 1961-1990. As indicated, similar results are obtained from the three methods. For the 1991-2002 period, the discharge values at JM, MQ and TNH decreased more than 20%. For period in the 21st century, the discharge changed with different trends in different catchments: a slight increase trend existed at JM, and a decrease trend existed at MQ

30   and TNH. The anthropic changes in the discharge estimated with the existing methods, $\Delta Q_h = \Delta Q - \Delta Q_c$,

17

was regarded as the partial of change induced by the change in the catchment specific parameter, ΔQ_w (see Sect. 3.2).

Our results show that both ΔQ_c and ΔQ_w are significant (Table 4). In general, ΔQ_w is positively related
5   with ΔQ and contributes more than half of the total absolute change. These results show that the change in the catchment parameter have an important role in the hydrological behaviors of the SRYR, which is similar to previous researches for the other catchments (Zheng et al., 2009, Zhao et al., 2009). A relative different result existed in the 21st century for the JM basin, where ΔQ was positive but ΔQ_w was negative and the climatic change, ΔQ_c became a dominant component in ΔQ.

10

If ΔQ_w is completely regarded as the human-induced change in the discharge (ΔQ_h), we obtain an unreasonable conclusion based on the results in Table 4; the human activities were able to cause significant negative impact on the hydrological processes in an area with a very low population density. This unreasonable conclusion indicates that something is missing from in the analysis. In fact, the
15   catchment specific parameter depends on several catchment properties (plants, permafrost, etc.) that can be influenced by climate change such as the changes in the precipitation, evapotranspiration and temperature (Yang et al., 2007; Williams et al., 2012; Jiang et al., 2015). Accordingly, Δw should not be completely referred to as the change in land use. Therefore, a further analysis is necessary to extract the impact of the climate change on ΔQ_w.

20   **4.2 Results of using Eq. (16)**

In this study, we first used the new method (Sect. 3.3) to investigate ΔQ_w with the regression formula Eq. (16). The w values for the three sub-basins obtained annually with different moving windows are shown in Figure 4. As indicated, an increase in the window's width can reduce the local oscillations (caused by the change in storage) of the time-w curves but will also remove more variation memories
25   by averaging all the Q, P and E_0 data. As indicated by Jiang et al. (2015), when the window width is larger than 10 years, the impact of the change in storage is sufficiently small to be assumed as negligible. Thus, the 11-year window is used to retain the maximum amount of information about temporal variability without having influence from a change in storage. Using an 11-year moving average method to remove changes in water storage is further verified by GRACE data for water
30   storage in the SRYR (details in Supplementary Material). Further, an 11-year average data were also used in previous studies (Jiang et al., 2015) and it matches the significant return period of streamflow data.

Changes in the moving average w values between 1965 and 2010 are shown in Figure 5(a) together
35   with the data points of the mean annual w values in different 11-year periods. The time-varying values of w in the three sub-basins significantly increased during 1980-2000. In the 21st century, this

increasing trend continued at MQ but stopped and transitioned to a decline trend for JM and TNH. MQ has the lowest dryness index (E_0/P) but its w value ranges between the w values of JM and TNH. Using these time-varying w data, the shift paths of the basin scale hydrology in the Budyko space can be plotted in Figure 5(b). Points in the Budyko space can be located respective to a given Budyko-type curve by changing the w value for Fu's equation. Example classical Budyko curves for w = 2.4,2.0 and 1.7 are shown in Fig. 5(b). The gray area of Fig. 5b indicates where the Budyko type-curve changes with different w values.The data points generally show a positive relationship between the evapotranspiration ratio (E/P) and E_0/P with slopes that are larger than the slope of traditional Budyko curves with a constant parameter. This is caused by the increase in w values with increasing E_0/P in the study area.

The parameter w in Fu's equation (Fu, 1981) represents an integrated effect of catchment properties (vegetation, soil properties and catchment topography, etc.) under a steady-state climate condition (Zhang et al., 2004; Yang et al., 2007; Williams et al., 2012). In this study, to investigate how the parameter of a basin responds to climate change, the relationship between the moving average w values and the climatic forces is analyzed with Eq. (15). Three optimal regression models (with the significance level of 0.001) were chosen through covariate analysis (Table 5). For different sub-basins, the selected variables in the respective model are not the same, but the explanatory variables contained in each model can be generally divided into two groups: water supply-related and energy supply-related. Water supply-related explanatory variables contain I or P, and the energy supply-related explanatory variables contain T or E_0. According to the Budyko hypothesis, the mean annual water balance in a basin is a synthesis of water supply from precipitation and energy supply-controlled loss of water by evapotranspiration. Both water supply-related and energy supply-related variables are included in each formula (Table 5), indicating the reasonability of the obtained results.

In general, both the annual precipitation (P) and the annual mean precipitation intensity (I) are negatively correlated to the w values but the correlation will be more significant when I is used in the formulas. E_0 and T are positive factors for the change in the w values. For the sub-basin JM, the air temperature (T) seems to be a more essential role than the potential evapotranspiration (E_0) in controlling the w value, which contrasts with that in MQ. In TNH, both T and E_0 are significant factors that correlated to the w value. For both of JM and TNH, Figure 4 and Figure 5 clearly shows that the w values of JM and TNH had an increase trend from 1990 to 2000 and a decline trend after 2000. This shift of the trends may be linked with the fact that during 1990-2000 the T value significantly increased (T is positively correlated with w) whereas after 2000 the T value was relatively steady but the I value significantly increased (I is negatively correlated with w).

To assess the impact of the change on the catchment parameter on at the basin scale discharge, Equation 21 was used to calculated ΔQ_c, where ΔQ_{c1} and ΔQ_{c2} were estimated with Eqs. (19) and (20), respectively. The change is related to the moving average data from 1966 with a window of 1961-1971. Results are shown in Figures 6 (a)-(c) where ΔQ, ΔQ_c, ΔQ_{c1} and ΔQ_{c2} are presented in the percentage of

5 the mean annual discharge during 1961-197. As indicated, ΔQ_c is close to ΔQ for the three sub-basins, demonstrating that the climate change is the primary cause of the discharge change in the SRYR. The absolute values of ΔQ_{c2} are generally higher than that of ΔQ_{c1}, indicating that the change in the catchment specific parameter plays a more important role than the direct impacts of the changes in the precipitation and potential evapotranspiration. The contribution of the catchment specific parameter

10 change obtained by existing methods (ΔQ_w) shown in Table 4 are similar with modified method ($\Delta Q - \Delta Q_{c1} \approx \Delta Q_{c2}$), which indicates that the modified method can obtain a time-vary results without expense of accuracy. However, existing methods attribute all catchment properties change impacts (ΔQ_w) to human activities (ΔQ_h). In JM and TNH, as shown in Figures 6 (a) and (b), the absolute ΔQ_{c2} value was higher than twice of the absolute ΔQ_{c1} value between 1988 and 2006. However, the anthropic

15 change in discharge could not be sufficiently estimated with $\Delta Q_h = \Delta Q - \Delta Q_c$ from these results, because the impact of the permafrost was not considered in Eq. (16).

4.3 Results of using Eq. (17)

The regression formula, Eq. (17), is more appropriate in comparison with Eq. (16) in this study because the study area is a cold region with permafrost. Substituting the results of Eq. (16) into Eq. (15), we

20 obtain the residual part of w as X. The need for using Eq. (17) can be indicated by the correlation between X and MFD, as shown in Figure 7. It is clear that X is positively correlated with MFD in JM ($R^2 = 0.58$, significance level <0.001) and in TNH ($R^2 = 0.47$, significance level <0.001). However, this X-MFD correlation is very weak in MQ. A higher average value of the MFD seems lead to a stronger correlation between the X and MFD.

25

According to the significant correlation between X and MFD in JM and TNH, a further stepwise regression analysis is carried out using Eq. (17) for JM and TNH, which leads to

$$w = 4.002 + 0.557\overline{T} - 2.237\overline{I} + 1.072\overline{D} \text{, for JM} \tag{26}$$

$$w = -1.782 + 0.523\overline{T} - 2.498\overline{I} + 4.665\overline{E}_0 + 0.954\overline{D} \text{, for TNH} \tag{27}$$

30 These regression formulas can increase the correlation coefficient to $R^2 = 0.92$ and $R^2 = 0.93$ for JM and TNH, respectively. The values of coefficient β_4 are positive and close to 1.0, indicating that MFD is a positive factor for the catchment parameter. Since MFD decreases with the degradation of permafrost, this positive relationship between w and MFD implies that the degradation of permafrost will cause negative changes in the w and E/P values and then increase the discharge in JM and TNH. Eqs. (26)

35 and (27) also show that the w value is positively correlated with the air temperature, T, and negatively correlated with the precipitation intensity, I, in both sub-basins and is positively correlated with E_0 in

20

TNH. These results of the relationship between the catchment parameter and the normal climatic forces are consistent with that shown in Table 5, but the values of the coefficients change.

Based on Eqs. (26) and (27), the results of ΔQ_{c1}, ΔQ_{c2} and ΔQ_c were estimated again with Eq. (17) for JM shown in Figure 6 (d) and TNH shown in Figure 6 (e). The moving average data of MFD for the sub-basins are limited to the period between 1966 and 2000 so that curves after 2000 are not shown in Figure 6 (d) and 6 (e). In comparison with the results of Eq. (16) shown in Figures 6 (a) and 6 (b), the difference between ΔQ and ΔQ_c in Figures 6 (d) and 6 (e) obviously decreases because most of the change in discharge are attributed to the climatic change. However, the time-varying patterns of ΔQ and ΔQ_c do not change much.

The anthropic derived change in discharge attributed is now estimated with $\Delta Q_h = \Delta Q - \Delta Q_c$ from the new results of ΔQ_c, as shown in Figure 8. As indicated, the anthropic change in discharge is generally less than 5% of the total change. Before 1990, the ΔQ_h values appear to show a random oscillation, which may not really indicate the anthropic change. After 1990, the ΔQ_h values in JM and TNH shown a long-term increase trend whereas the ΔQ_h values in MQ shown a negative trend. These trends may be linked with the environment conservation program implemented in the 1990s the SRYR but it is not clear for that why MQ shown different trend from that in JM and TNH.

5 Discussions

5.1 Controls of the change in MFD

In Sect. 4.3 we found that the catchment parameter (w) in JM and TNH is correlated with MFD and roles as an influence factor for the discharge in additional to the normal climatic factors. Questions arise here with the relationship: what controls the change in MDF? Is the MDF value depends on the air temperature that have been included in Sect. 4.2?

It was well known that global warming has triggered degradation of the cryosphere, including glaciers and permafrost in the Tibetan Plateau. Such a relationship is exhibited in Figure 2 where MFD generally decreased in the study period whereas the air temperature shown an increase trend. To analyse this correlation, we compared the MFD data for 11 stations with the annual mean air temperature (MAT) and the cold season (from October to March) mean air temperature (CMAT). Locations of these stations are shown in Figure 1b and the correlation analysis results are shown in Table 6. In general, the significance of the correlation between MFD and CMAT is higher than the correlation between MFD and MAT, except for two stations (M8, M11) where the record lengths were less than 15 years. This indicates that the decrease in MFD may be controlled by the increase in the air temperature in the cold seasons. However, the R-squared correlation coefficients are not high,

indicating that the region may be influenced by other factors such as the soil temperature and moisture, snowpack and canopy (Goodrich, 1982; Nelson et al., 1997; Yamazaki et al., 1998; Shanley and Chalmers, 1999). However, at present it is difficult to quantitatively assess the impacts of these factors because the lack of data.

5

If the negative correlation between the MFD and MAT is significant, it will influence the meaning of the regression formulas for the catchment parameter, w, as is presented in Table 5 and Eqs. (26) and (27). According to Eqs. (26) and (27), w can be determined by

$$w = w_f + \beta_3 \overline{T} + \beta_4 \overline{D} \tag{28}$$

10   where w_f is the components related to the other factors, β_3 and β_4 are the coefficients for the MAT and MFD (both are positive), respectively. Further, we can describe the MFD-MAT correlation as

$$\overline{D} = -\xi \overline{T} + \eta \tag{29}$$

where ξ is the absolute slope of the correlation line and η is the residual resulting from other controls. Substituting Eq. (29) into Eq. (28) yields

15

$$w = \left(w_f + \beta_4 \eta\right) + \left(\beta_3 - \beta_4 \xi\right)\overline{T} \tag{30}$$

Because β_3, β_4 and ξ are positive coefficients, then $\beta_3 - \beta_4 \xi$ must be less than β_3. Accordingly, the MFD-MAT correlation may reduce positive sensitivity (when ξ is less than β_3/β_4) or cause negative sensitivity (when ξ is higher than β_3/β_4) of the catchment parameter to the change in the air temperature. This may explain why the coefficient of T in Table 5 is less than that of Eqs. (26) and (27).

20

If $\beta_3 \approx \beta_4 \xi$, then the role of MAT cannot be explicitly included in Eq. (30). This may be the reason why T is not included in the formulas of the sub-basin MQ in Table 5 though the effects of the air temperature should also exist in the basin. Such an effect could also be applied to explain why the relation between X and MFD is weak in MQ (Figure 7). It is speculated that in MQ the w value is also
25   positively correlated with MFD but is offset by the effect of air temperature. In general, the increasing air temperature will increase evapotranspiration and decrease the discharge in catchments without permafrost (Yang and Yang, 2011; Tang et al., 2012). However, in the cold Tibetan plateau region, the degradation of permafrost due to increasing air temperature can enlarge the discharge of groundwater and partially counteract the negative impact of the increasing air temperature (McKenzie *et al.*, 2013).
30   This particular effect leads to a more complex response of streamflow in the cold basins with permafrost than that in warm basins without permafrost.

5.2 Remarks

This study does not directly consider permafrost degradation as a major research objective in understanding the linkages between climate change and runoff generation at the catchment scale. It is different from previous studies which regard permafrost as a main research object with subsurface domain. Most of the previous research about permafrost degradation highlight temperature increase impacts on permafrost degradation, leading to changes in soil physical properties, groundwater storage, and discharge. However, these changes are focused on the subsurface domain, rather than at the catchment scale. In these previous studies, changes in the interactions between subsurface and surface conditions (e.g. evaporation, precipitation, and precipitation intensity) are neglected. Considering the complex impact of permafrost degradation at the catchment scale on the hydrological system, it is necessary to account for this process to better understand and predict change. At present, there are few physical models that can accurately assess these situations; we demonstrate that these changes can be preliminarily considered using conceptual models and statistic methods. Through this modified analysis method, climate change directly impacts (ΔQ_{c1}) are calculated based on existing method, potential climate impacts (ΔQ_{c2}) are analysed by a stepwise linear regression analysis between catchment parameters and potential candidate variables. This method efficiently considered climate change impacts on catchment properties which provide a more reasonable assessment of human activity impacts. With this flexible method all potential factors can be considered in discharge change analysis by stepwise regression analysis, the residual errors of regression analysis possibly indicate impacts of the penitential factors which wasn't directly considered in regression analysis due to record limitation. An important finding from our research is that by considering permafrost at the catchment hydrological scale, degrading permafrost is a positive factor for discharge change.

In this study, we highlight the role of the permafrost degradation with global warming in the change of discharge in the SRYR because the catchment parameter (w) is positively correlated with the MFD. An increasing trend in MFD implies a decreasing trend in permafrost. However, the MFD is not a full measurement on the thickness (or volume) of the permafrost which only represents the surficial part of the permafrost. We could not avoid this limitation because the direct observation data of the varying thickness for the permafrost are not available. Observation of the MFD is also difficult and limited in a few observation stations. In each of the three studied basins, we chose one observation station to extract the representative MFD data for the correlation analysis. This is sufficient to capture the general relationship but may induce quantitative errors because the distributed patterns of the MFD are not considered. It is possible to use several geophysical methods in characterizing distributed frozen depth of shallow soils, such as: electrical resistivity imaging, electromagnetic induction, ground penetrating radar and infrared imaging (Briggs et al., 2016). However, these methods could only be performed in a small area (the size is generally less than 1 km) and are too expensive to be applied everywhere within a larger catchment.

An unresolved question is why does the decreasing MFD act as a positive factor for the discharge of basins in the SRYR? This is still an unsolved problem that was not resolved with only the Budyko framework. However, potential physical explanations can be found in previous studies. It has been found that the permafrost degradation could enlarge baseflow in cold regions (Walvoord and Striegl, 2007; Jacques and Sauchyn, 2009; Bense et al., 2012; Evans et al., 2015; Duan et al.,2017). Decrease in MFD because of global warming was considered as a major factor for the increase in baseflow in the Qilian mountain, China (Qin et al. 2016). Additionally, the melt ice within permafrost and increasing hydrologic connectivity fallowing permafrost thaw-induced land-cover change will increase the runoff discharge (Connon et al. 2014; Duan et al. 2017). According to these research, further deeper investigations are required to link the rainfall-runoff and base flow behaviours with the physical mechanism of frozen soils and performed in the SRYR.

There are also potential limitations in the data processing. We extracted the annual data of P, E_0, T and I for the three sub-basins from the gridded data of IDW interpolation. Among them, the precipitation data agree with the TRMM 3B42 data, indicating the efficiency of the IDW method. However, it is difficult to assess how the elevation-dependent variations of P, E_0, T and I were sufficiently included in the IDW interpolation. Quantitative analyses of the elevation effects on these meteorological factors are very limited in the literature. The elevation effects could be partly dealt with many distributed weather stations (Figure 1b). The influences of the local topographic relief of the ground surface in a sub-basin were expected to be counteracted at the catchment scale and nonsignificant for the time-varying patterns. Nevertheless, it is an essential problem which requires much more investigation in further studies. Another problem involves the normalization of data in the regression analysis. In Eqs. (15)-(17), $\overline{T}\ (=T/T_m)$ is normalized with T_m where T_m are not close to zero. This is because a very small T_m value could significantly enlarge the relative change in T and increase the errors in estimating Δw. Since the objective is to estimate a dimensionless change, a larger value of T_m can be used if the mean annual air temperature is close to zero.

6. Conclusions

This work modifies and improves on the traditional separation approach to identify the contribution of climate change to the change in discharge of drainage basins. This modified approach is applied for the source region of the Yellow River (SRYR) in analyzing the inter-annual change in discharge for a past 50 years. The role of varying permafrost in this cold region is investigated by using the observation data of the maximum frozen depth. According to the obtained results, several conclusions can be highlighted:

(1) The change in discharge of the SRYR in the past half-century is mainly controlled by the climate change rather than the local human activities. In the 1990s, a significant decrease in discharge was triggered by the increase of the air temperature and the decrease of the annual precipitation. In

comparison with the annual precipitation, the precipitation intensity is a stronger control of the discharge in the SRYR.

(2) Analysis of the inter-annual water balance with Fu's formula in the Budyko framework shows a positive relationship between the catchment specific parameter and the aridity index. The change in the
5 catchment specific parameter, w, is interpreted to be due to climate change and not land use change, differing from previous research. Moreover, in two permafrost widely covered sub-basins the catchment specific parameter is correlated with the maximum frozen depth, which indicates the impact of the permafrost on discharge behaviors.

(3) The negative correlation between the maximum frozen depth and air temperature indicates the
10 impact of global warming on permafrost degradation but implies conflicting effects of the air temperature rising on the discharge. The increasing air temperature is generally a negative force for discharge. However, in our cold study area it also causes degrading permafrost that can act as a positive factor for discharge. Such conflicting effects enhance the uncertainty in assessments of the hydrological response to climate change in the SRYR.

15

References

Abdul Aziz, O. I., & Burn, D. H. (2006). Trends and variability in the hydrological regime of the
25   Mackenzie River Basin. Journal of Hydrology, 319(1-4), 282-294. doi: 10.1016/j.jhydrol.2005.06.039

Allen, R., L.S. Pereira, D. Raes, & M. Smith. (1998). Crop evapotranspiration – Guidelines for computing crop water requirements. FAO Irrigation and Drainage PaperN° 56. Rome, Italy.

30 Arora, V. K. (2002). The use of the aridity index to assess climate change effect on annual runoff. Journal of Hydrology, 265(s 1–4), 164-177.

Bense, V. F., Kooi, H., Ferguson, G., & Read, T. (2012). Permafrost degradation as a control on hydrogeological regime shifts in a warming climate. Journal of Geophysical Research Earth Surface, 117(F3), 8316.

Birsan, M.-V., Molnar, P., Burlando, P., & Pfaundler, M. (2005). Streamflow trends in Switzerland. Journal of Hydrology, 314(1-4), 312-329. doi: 10.1016/j.jhydrol.2005.06.008

Briggs, M. A., Campbell, S., Nolan, J., Walvoord, M. A., Ntarlagiannis, D., & Day-Lewis, F. D., et al. (2016). Surface geophysical methods for characterising frozen ground in transitional permafrost landscapes. Permafrost & Periglacial Processes.

Cheng, G., & Wu, T. (2007). Responses of permafrost to climate change and their environmental significance, Qinghai‑Tibet Plateau. Journal of Geophysical Research Atmospheres, 112(112), 93-104.

Chen, J., Wu, X., Finlayson, B. L., Webber, M., Wei, T., Li, M., & Chen, Z. (2014). Variability and trend in the hydrology of the Yangtze River, China: Annual precipitation and runoff. Journal of Hydrology, 513, 403-412. doi: 10.1016/j.jhydrol.2014.03.044

Chiew, F. H. S., Teng, J., Vaze, J., Post, D. A., Perraud, J. M., Kirono, D. G. C., & Viney, N. R. (2009). Estimating climate change impact on runoff across southeast Australia: Method, results, and implications of the modeling method. Water Resources Research, 45(10), n/a-n/a. doi: 10.1029/2008wr007338

Choudhury, B. J. (1999), Evaluation of an empirical equation for annual evaporation using field observations and results from a biophysical model. J. Hydrol., 216, 99–110.

Cuo, L., Zhang, Y., Gao, Y., Hao, Z., & Cairang, L. (2013). The impacts of climate change and land cover/use transition on the hydrology in the upper Yellow River Basin, China. Journal of Hydrology, 502, 37-52. doi: 10.1016/j.jhydrol.2013.08.003

Cuo, L., Zhang, Y., Bohn, T. J., Zhao, L., Li, J., & Liu, Q., et al. (2015). Frozen soil degradation and its effects on surface hydrology in the northern tibetan plateau. Journal of Geophysical Research Atmospheres, 120(16).

Donohue, R. J., Roderick, M. L., & Mcvicar, T. R. (2012). Roots, storms and soil pores: incorporating key ecohydrological processes into budyko's hydrological model. Journal of Hydrology, 436-437, 35-50.

Duan, L., Man, X., Kurylyk, B. L., & Cai, T. (2017). Increasing winter baseflow in response to permafrost thaw and precipitation regime shifts in northeastern china. Water, 9(1), 1-15.

Duan, L., Man, X., Kurylyk, B. L., Cai, T., & Li, Q. (2017). Distinguishing streamflow trends caused by changes in climate, forest cover, and permafrost in a large watershed in northeastern china. Hydrological Processes, 31(10).

Frampton, A., Painter, S., Lyon, S. W., & Destouni, G. (2011). Non-isothermal, three-phase simulations of near-surface flows in a model permafrost system under seasonal variability and climate change. Journal of Hydrology, 403(3-4), 352-359. doi: 10.1016/j.jhydrol.2011.04.010

Fu, B. P. (1981), On the calculation of the evaporation from land surface (in Chinese), Sci. Atmos. Sin., 5, 23–31.

Goodrich, L. E. (1982). The influence of snow cover on the ground thermal regime. Canadian Geotechnical Journal, 19(4), 421-432.

Hair J.F.J., Anderson R.E., Tatham R.L., & Black W.C. (1995) Multivariate Data Analysis. New York: Macmillan.

Hao, Z. C., Tong, K., Liu, X. L., & Zhang, L. L. (2014). Capability of tmpa products to simulate streamflow in Upper Yellow and Yangtze River basins on Tibetan Plateau. Water Science and Engineering, 7(3), 237-249.

Hu, Y., Maskey, S., Uhlenbrook, S., & Zhao, H. (2011). Streamflow trends and climate linkages in the source region of the Yellow River, China. Hydrological Processes, 25(22), 3399-3411. doi: 10.1002/hyp.8069

Immerzeel, W. W., van Beek, L. P., & Bierkens, M. F. (2010). Climate change will affect the Asian water towers. Science, 328(5984), 1382-1385. doi: 10.1126/science.1183188

IPCC (2007). Climate change 2007: The Physical Science Basis. In: Contribution of Working Group I to the Fourth Assessment Report of the Intergovernmental Panel on Climate Change, Cambridge University Press, Cambridge, 996 pp.

Jacques, J. M. S., & Sauchyn, D. J. (2009). Increasing winter baseflow and mean annual streamflow from possible permafrost thawing in the northwest territories, canada. Geophysical Research Letters, 36(1), 329-342.

Jiang, C., Xiong, L., Wang, D., Liu, P., Guo, S., & Xu, C.-Y. (2015). Separating the impacts of climate change and human activities on runoff using the Budyko-type equations with time-varying parameters. Journal of Hydrology, 522, 326-338. doi: 10.1016/j.jhydrol.2014.12.060

Jin, H. J., Wang, S. L., Lan-Zhi, L., Rui-Xia, H. E., Chang, X. L., & Luo, D. L. (2010). Features and degradation of frozen ground in the sources area of the Yellow River, China. Journal of Glaciology & Geocryology,49(12), 5522-9. (in Chinese with English abstract)

Jolliffe IT (2002) Principal components in regression analysis. Principal Component Analysis: 167–198.

Jou, Y. J., & Cho, H. J. (2014). A VIF-based optimization model to alleviate collinearity problems in multiple linear regression. Kluwer Academic Publishers.

Kuhnel, V., J. C. I. Dooge, J. C. I. O'Kane, and R. J. Romanowicz (1991), Partial analysis applied to scale problems in surface moisture fluxes, Surv. Geophys., 12, 221– 247, doi:10.1007/BF01903420.

Kurylyk, B. L., MacQuarrie, K. T., & McKenzie, J. M. (2014). Climate change impacts on groundwater and soil temperatures in cold and temperate regions: Implications, mathematical theory, and emerging simulation tools. Earth-Science Reviews, 138, 313-334.

Lan, Y., Zhao, G., Zhang, Y., Wen, J., Liu, J., & Hu, X. (2010). Response of runoff in the source region of the Yellow River to climate warming. Quaternary International, 226(1-2), 60-65. doi: 10.1016/j.quaint.2010.03.006

Liang, L., Li, L., Liu, C., & Cuo, L. (2013). Climate change in the Tibetan Plateau Three Rivers Source Region: 1960-2009. International Journal of Climatology, 33(13), 2900-2916. doi: 10.1002/joc.3642

Liang, S., Ge, S., Wan, L., & Zhang, J. (2010). Can climate change cause the Yellow River to dry up? Water Resources Research, 46(2), n/a-n/a. doi: 10.1029/2009wr007971

Liu, C., & Zheng, H. (2004). Changes in components of the hydrological cycle in the yellow river basin during the second half of the 20th century. Hydrological Processes, 18(12), 2337-2345.Introduction

Luo, D., HuiJun, J., Marchenko, S., & Romanovsky, V. (2014a). Distribution and changes of active layer thickness (ALT) and soil temperature (TTOP) in the source km2 of the Yellow River using the GIPL model. Science China Earth Sciences, 57(8), 1834-1845. doi: 10.1007/s11430-014-4852-1

Luo, D., Jin, H., Lü, L., & Wu, Q. (2014b). Spatiotemporal characteristics of freezing and thawing of the active layer in the source areas of the Yellow River (SAYR). Chinese Science Bulletin, 59(24), 3034-3045. doi: 10.1007/s11434-014-0189-6

Lyon, S. W., & Destouni, G. (2010). Changes in Catchment-Scale Recession Flow Properties in Response to Permafrost Thawing in the Yukon River Basin. International Journal of Climatology, 30(14), 2138-2145. doi: 10.1002/joc.1993

Lyon, S. W., Destouni, G., Giesler, R., Humborg, C., Mörth, M., Seibert, J., . . . Troch, P. A. (2009). Estimation of permafrost thawing rates in a sub-arctic catchment using recession flow analysis. Hydrology and Earth System Sciences Discussions, 6(1), 63-83. doi: 10.5194/hessd-6-63-2009

Ma, Z., Kang, S., Zhang, L., Tong, L., & Su, X. (2008). Analysis of impacts of climate variability and human activity on streamflow for a river basin in arid region of northwest china. Journal of Hydrology, 352(3–4), 239-249.

McKenzie, J.M., C.I. Voss, 2013. Permafrost thaw in a nested groundwater-flow system. Hydrogeology Journal, DOI: 10.1007/s10040-012-0942-3.Meng, F., Su, F., Yang, D., Tong, K., & Hao, Z. (2016). Impacts of recent climate change on the hydrology in the source region of the Yellow River basin. Journal of Hydrology: Regional Studies, 6, 66-81. doi: 10.1016/j.ejrh.2016.03.003

Nelson, F. E., Shiklomanov, N. I., and Mueller, G. R. (1997). Estimating active layer thickness over a large region: Kaparuk River basin, Alaska, USA, Arctic Alpine Res., 29, 367–378.

Neter J, Wasserman W, Kutner MH (1989) Applied Linear Regression Models. Homewood, IL: Irwin.

Ol'dekop, E. M. (1911), On evaporation from the surface of river basins: Transactions on Meteorological Observations, Lur-evskogo (in Russian),report, Univ. of Tartu, Tartu, Estonia

Qin, Y., Lei, H., Yang, D., Gao, B., Wang, Y., & Cong, Z., et al. (2016). Long-term change in the depth of seasonally frozen ground and its ecohydrological impacts in the Qilian Mountains, northeastern Tibetan Plateau. Journal of Hydrology, doi:10.1016/j.jhydrol.2016.09.008

Ren, L. I., Zhao, L., Ding, Y. J., Shen, Y. P., Er-Ji, D. U., & Liu, G. Y. (2009). The effect of global radiation budget on seasonal frozen depth in the Tibetan Plateau. Journal of Glaciology & Geocryology, 31(3), 422-430. (in Chinese)

Ran, Y., Li, X., Cheng, G., Zhang, T., Wu, Q., & Jin, H., et al. (2012). Distribution of permafrost in china: an overview of existing permafrost maps. Permafrost & Periglacial Processes, 23(4), 322-333.

Roderick, M. L., & Farquhar, G. D. (2011). A simple framework for relating variations in runoff to variations in climatic conditions and catchment properties. Water Resources Research, 47(12), n/a-n/a. doi: 10.1029/2010wr009826

Sankarasubramanian, A., Vogel, R. M., & Limbrunner, J. F. (2001). Climate elasticity of streamflow in the united states. Water Resources Research,37(6), 1771-1781

Schaake, J. C., & C. Liu (1989), Development and application of simplewater balance models to understand the relationship between climate andwater resources, in New Directions for Surface Water Modeling, IAHSPubl. Ser., vol. 181, edited by M. L. Kawas, pp. 343–352, Int. Assoc.of Hydrol. Sci., Oxford, U. K.

Schaake, J. C. (1990), From climate to flow, in Climate Change and U.S. Water Resources, edited by P. E. Waggoner, chap. 8, pp. 177–206, John Wiley, New York.

Schreiber, P. (1904), Über die Beziehungen zwischen dem Niederschlagund der Wasserführung der Flüße in Mitteleuropa, Z. Meteorol.,21(10), 441–452. Sci. Atmos. Sin., 5, 23–31, 1981. (in Chinese)

Shanley, J. B., & Chalmers, A. (1999). The effect of frozen soil on snowmelt runoff at sleepers river, vermont. Hydrological Processes, 13(12-13), 1843–1857.

Su, F., Zhang, L., Ou, T., Chen, D., Yao, T., Tong, K., & Qi, Y. (2016). Hydrological response to future climate changes for the major upstream river basins in the Tibetan Plateau. Global and Planetary Change, 136, 82-95. doi: 10.1016/j.gloplacha.2015.10.012

Tang, C., Crosby, B. T., Wheaton, J. M., & Piechota, T. C. (2012). Assessing streamflow sensitivity to temperature increases in the salmon river basin, Idaho. Global & Planetary Change, s 88–89(s 88–89), 32-44

Tang, Y., Tang, Q., Tian, F., Zhang, Z., & Liu, G. (2013). Responses of natural runoff to recent climatic variations in the Yellow River basin, China. Hydrology and Earth System Sciences, 17(11), 4471-4480. doi: 10.5194/hess-17-4471-2013

Tong, K., Su, F., Yang, D., & Hao, Z. (2014). Evaluation of satellite precipitation retrievals and their potential utilities in hydrologic modelling over the Tibetan Plateau. Journal of Hydrology, 519([C@213fee), 423-437.

Walvoord, M. A., & Striegl, R. G. (2007). Increased groundwater to stream discharge from permafrost thawing in the Yukon River basin: potential impacts on lateral export of carbon and nitrogen. Geophysical Research Letters, 34(12), 123–134.

Wang Tao Editor. (2006). 1:4000000 Map of the Glaciers, Frozen Ground and Deserts in China. Beijing: Science Press.

Wang, D., & Hejazi, M. (2011). Quantifying the relative contribution of the climate and direct human impacts on mean annual streamflow in the contiguous United States. Water Resources Research, 47(9), 411.

Wang, S.-Y., Liu, J.-S., & Ma, T.-B. (2010). Dynamics and changes in spatial patterns of land use in Yellow River Basin, China. Land Use Policy, 27(2), 313-323. doi: 10.1016/j.landusepol.2009.04.002

Wang, X. (2014). Advances in separating effects of climate variability and human activity on stream discharge: An overview. Advances in Water Resources, 71, 209-218. doi: 10.1016/j.advwatres.2014.06.007

Xiong, L., & Guo, S. (2012). Appraisal of Budyko formula in calculating long-term water balance in humid watersheds of southern China. Hydrological Processes, 26(26), 1370-1378.

Yang, D., Li, C., Hu, H., Lei, Z., Yang, S., Kusuda, T., & Musiake, K. (2004). Analysis of water resources variability in the Yellow River of China during the last half century using historical data. Water Resources Research, 40(6), n/a-n/a. doi: 10.1029/2003wr002763

Yang, H., & Yang, D. (2011). Derivation of climate elasticity of runoff to assess the effects of climate change on annual runoff. Water Resources Research, 47(7), 197-203.

Yang, H., Yang, D., & Hu, Q. (2014). An error analysis of the Budyko hypothesis for assessing the contribution of climate change to runoff. Water Resources Research, 50(12), 9620–9629.

Yang, H., Yang, D., Lei, Z., & Sun, F. (2008). New analytical derivation of the mean annual water-energy balance equation. Water Resources Research, 44(3), n/a-n/a. doi: 10.1029/2007wr006135

Zhang, L., Hickel, K., Dawes, W. R., Chiew, F. H. S., Western, A. W., & Briggs, P. R. (2004). A rational function approach for estimating mean annual evapotranspiration. Water Resources Research, 40(2), n/a-n/a. doi: 10.1029/2003wr002710

5   Zhang, Q., Xu, C.-Y., & Yang, T. (2008). Variability of Water Resource in the Yellow River Basin of Past 50 Years, China. Water Resources Management, 23(6), 1157-1170. doi: 10.1007/s11269-008-9320-2

Zhao, F., Xu, Z., Zhang, L., & Zuo, D. (2009). Streamflow response to climate variability and human activities in the upper catchment of the Yellow River Basin. Science in China Series E: Technological Sciences, 52(11), 3249-3256. doi: 10.1007/s11431-009-0354-3

10 Zheng, H., Zhang, L., Liu, C., Shao, Q., & Fukushima, Y. (2007). Changes in stream flow regime in headwater catchments of the Yellow River basin since the 1950s. Hydrological Processes, 21(7), 886-893. doi: 10.1002/hyp.6280

Zheng, H., Zhang, L., Zhu, R., Liu, C., Sato, Y., & Fukushima, Y. (2009). Responses of streamflow to climate and land surface change in the headwaters of the Yellow River Basin. Water Resources
15 Research, 45. doi: 10.1029/2007wr006665

Zhou, Y., Guo, D., Qiu, G. and Cheng, G. (2000) Geocryology in China. Science Press, Beijing, 450p. (in Chinese)
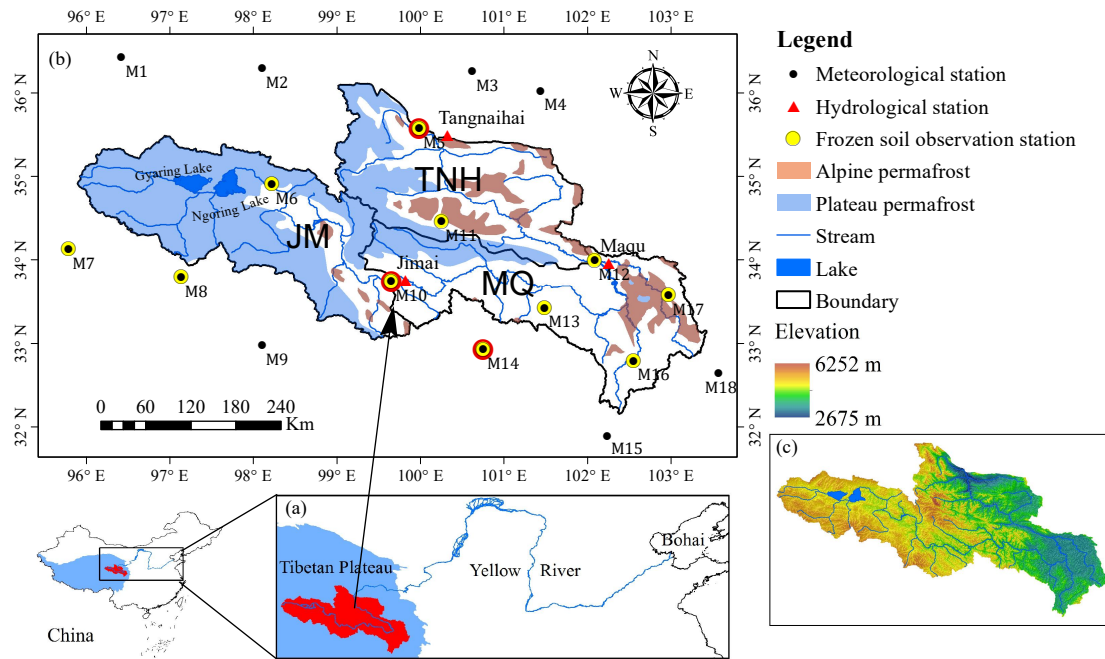
Figure 1 (a) Location map of the source region of the Yellow River (JM, MQ and TNH) (b) Distribution of permafrost, meteorological and hydrological stations (The red circles indicates stations which have the longest frozen soil record in the respective sub-basin.). (c) Elevation of the study area.
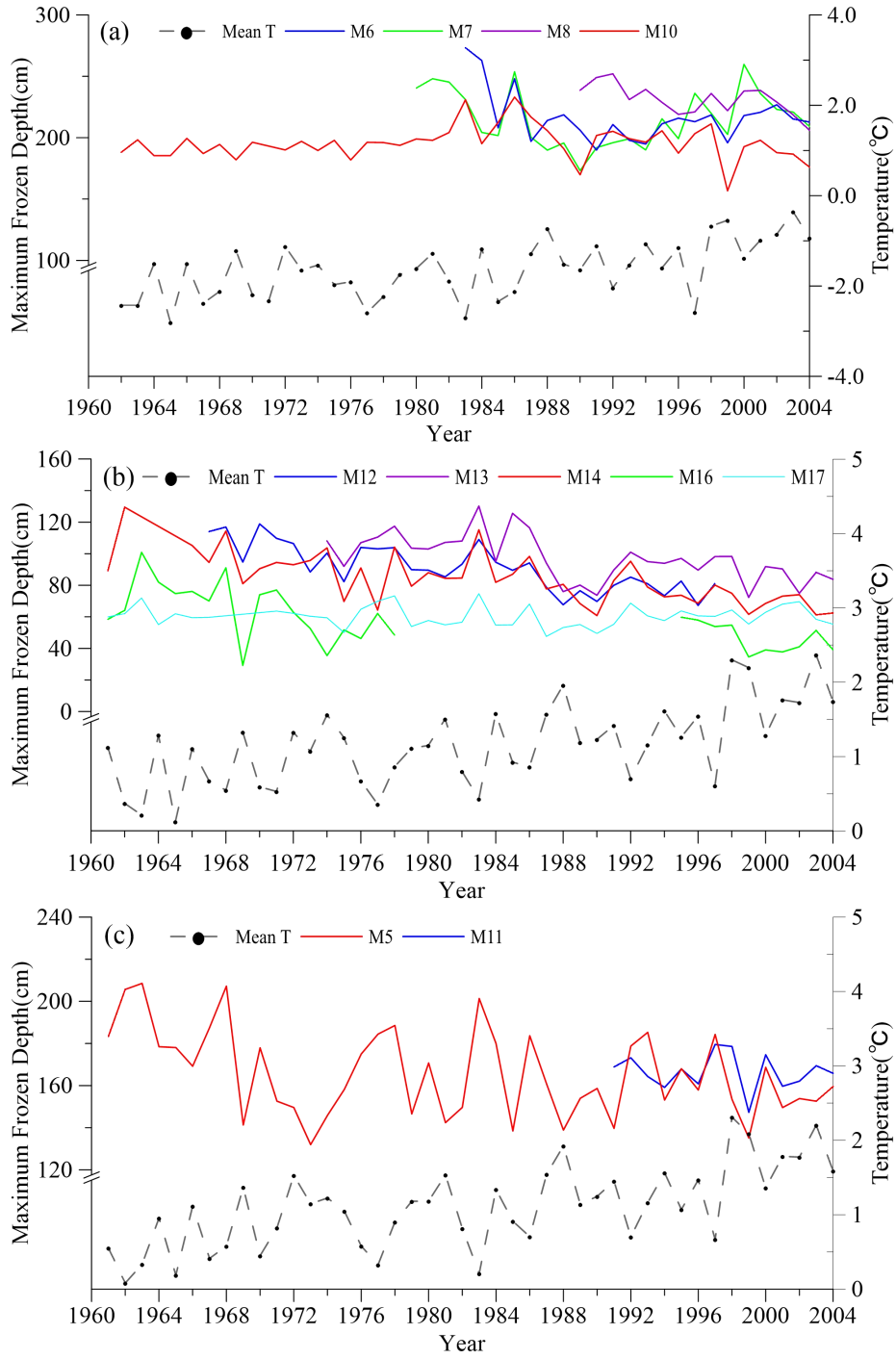
Figure 2 Change in the maximum frozen depth (MFD) and annual mean temperature of (a) JM, (b) MQ and (c) TNH subbasins.
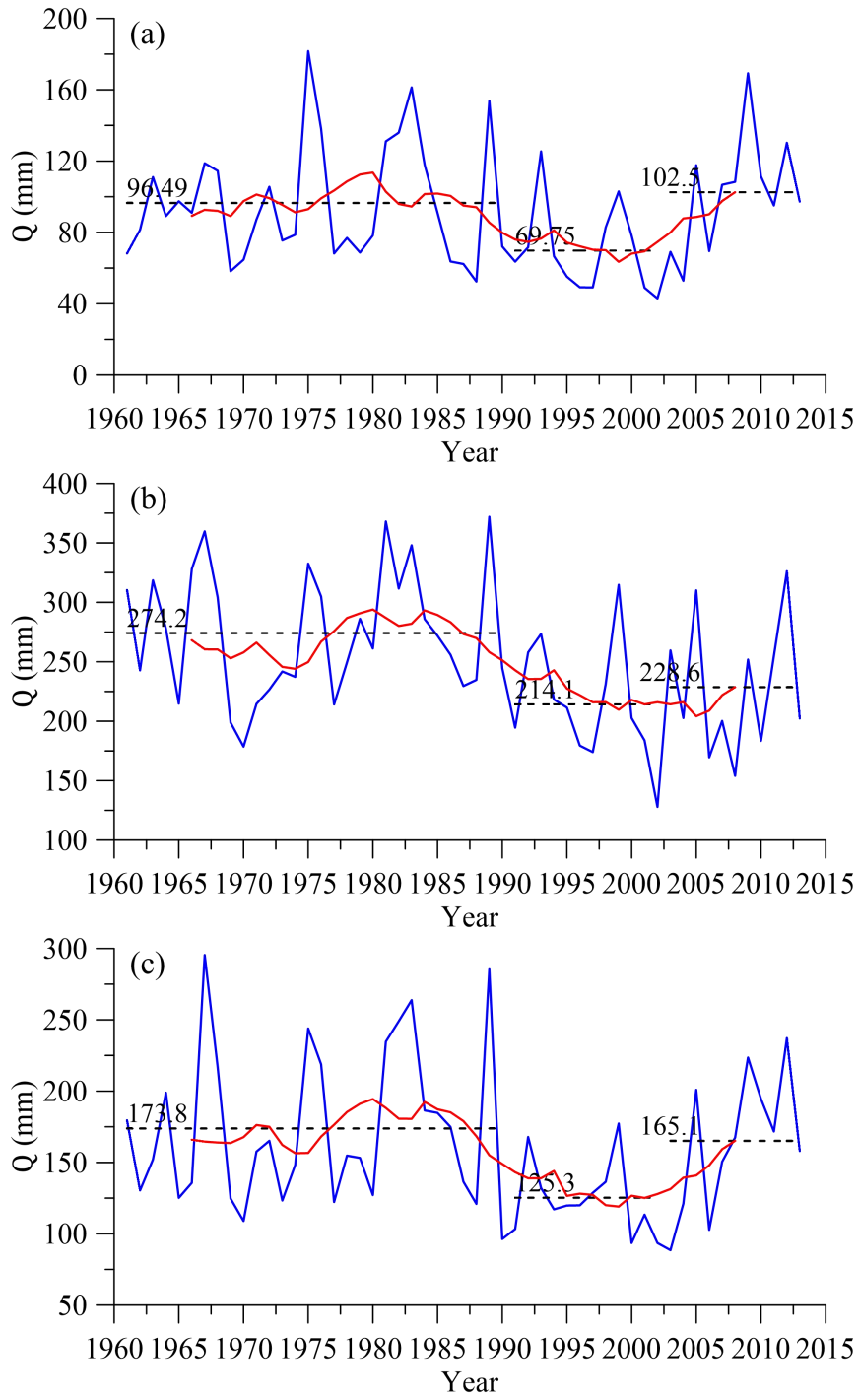
Figure 3 Time series of annual discharge, *Q*, in (a) JM, (b) MQ, and (c) TNH. The dashed line, red line and blue line indicate the mean value in different periods, 11-year moving average value and annual mean value of discharge, respectively.

34
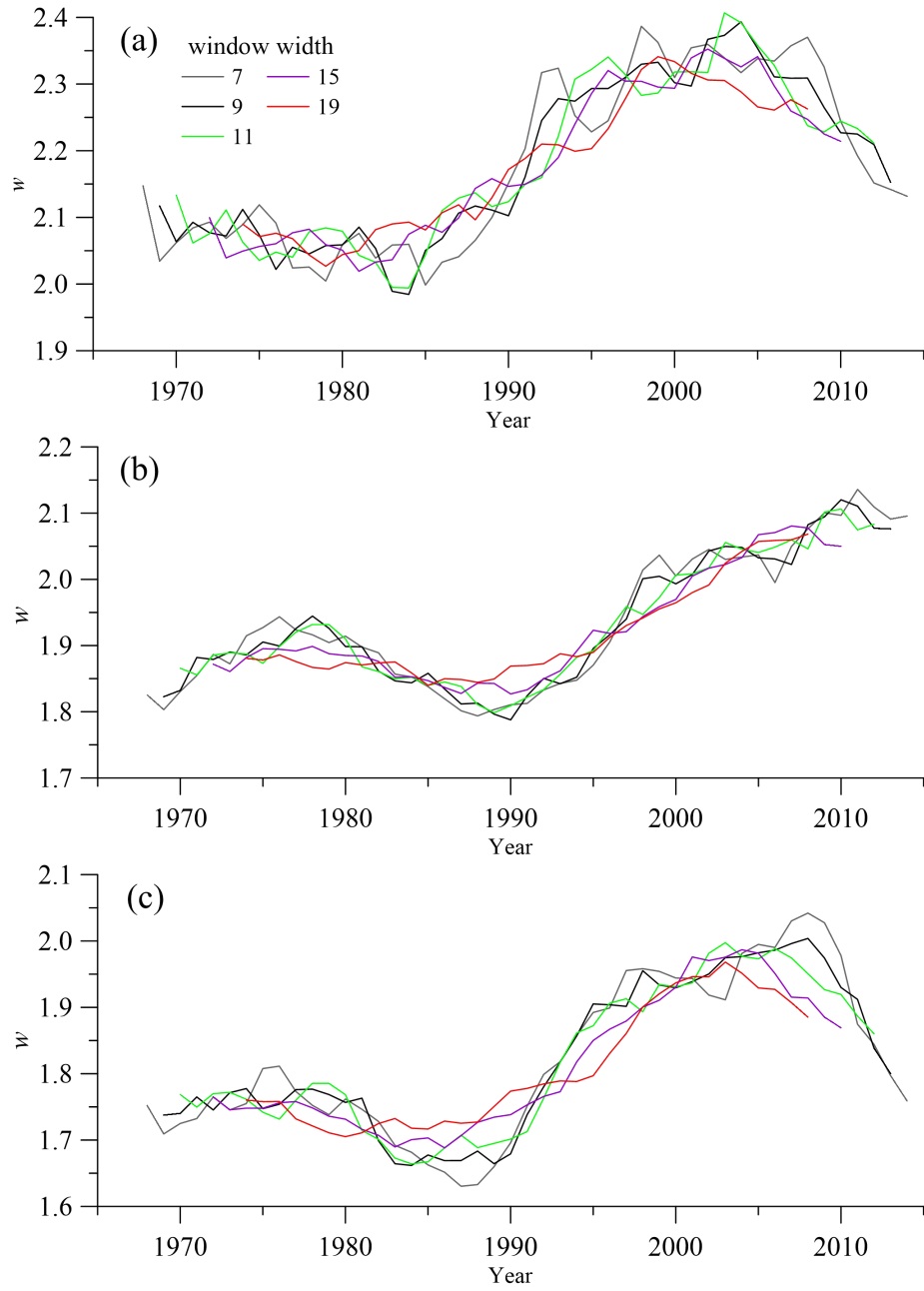
Figure 4 Time series of the catchment parameter (w) obtained from different widths of the moving windows for JM (a), MQ (b) and TNH(c).
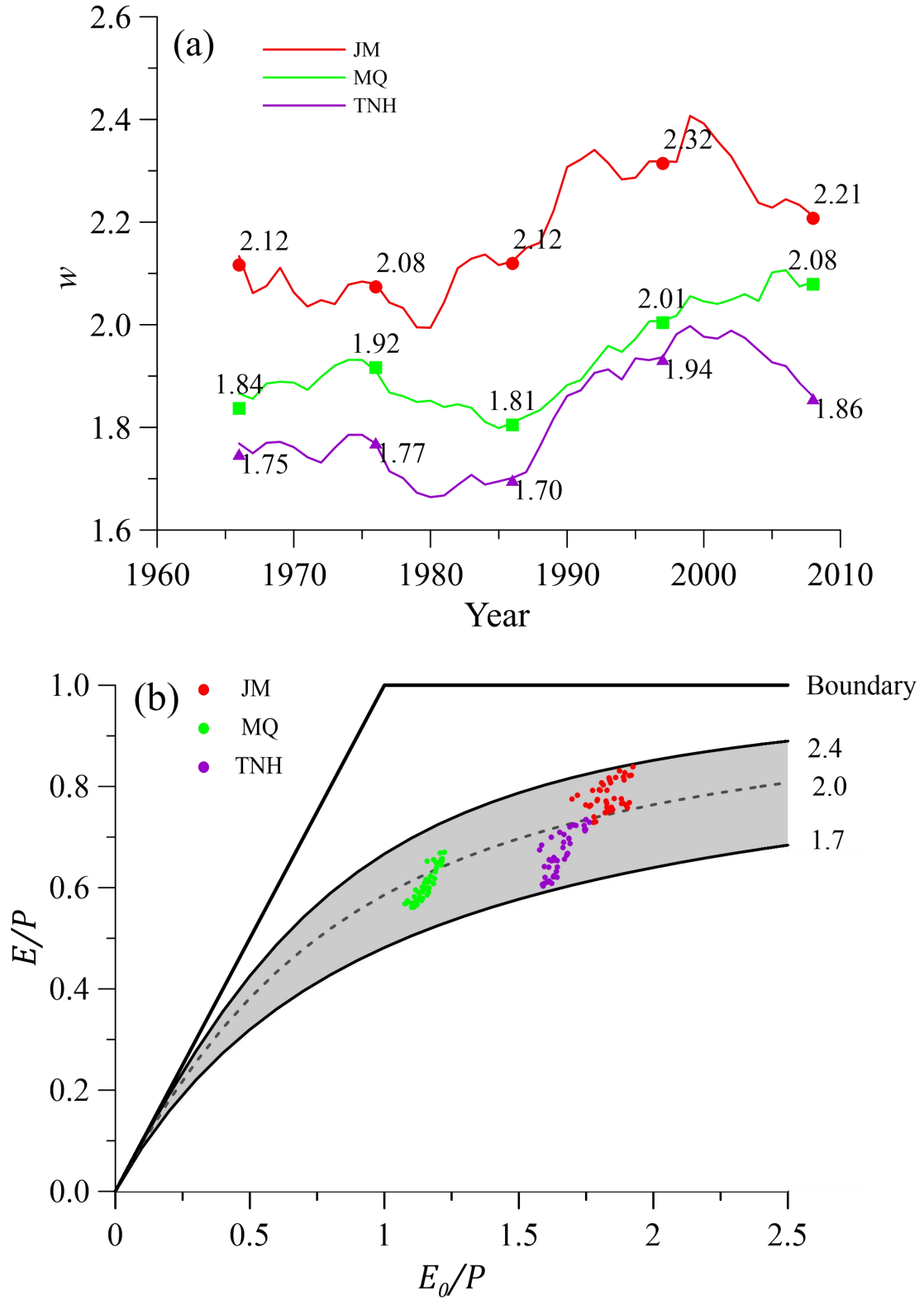
Figure 5 Time-varying values of the catchment parameter (*w*) in Fu's formula (a) and plots of the moving average water balance in the Budyko space (b) for the three sub-basins. The labelled points in (a) show the mean annual *w* values for different periods (1961-1970, 1971-1980, 1981-1991, 1992-2002, 2003-2013) which are plotted for the mid-point of the time periods. In (b), 2.4, 2.0 and 1.7 refer to the *w* value for the three type curves.
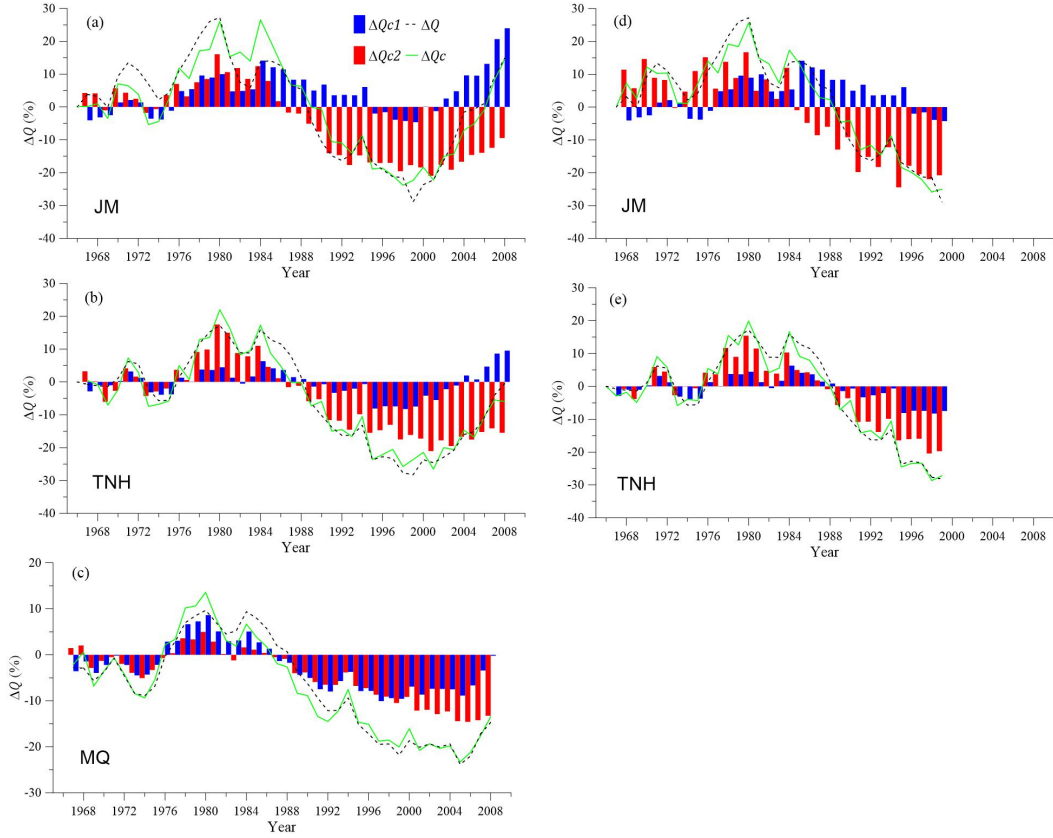
Figure 6 Decomposition results of the climatic change in discharge (ΔQ_{c1}, ΔQ_{c2} and ΔQ_c) in comparison with the total change in discharge (ΔQ) for the sub-basins. (a), (b) and (c) are the results of using Eq. (16) for JM, TNH and MQ, respectively. (d) and (e) are the results of using Eq. (17) for JM and TNH, respectively.
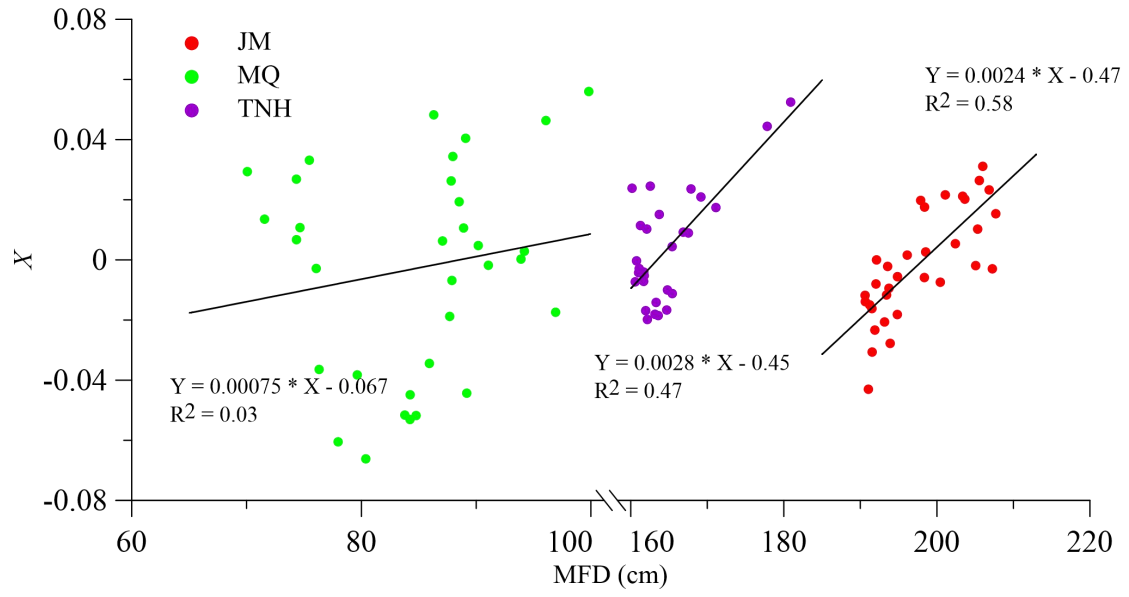
Figure 7 Correlation between X and the maximum frozen depth (MFD). The X values are estimated using Eqs. (15) and (16).
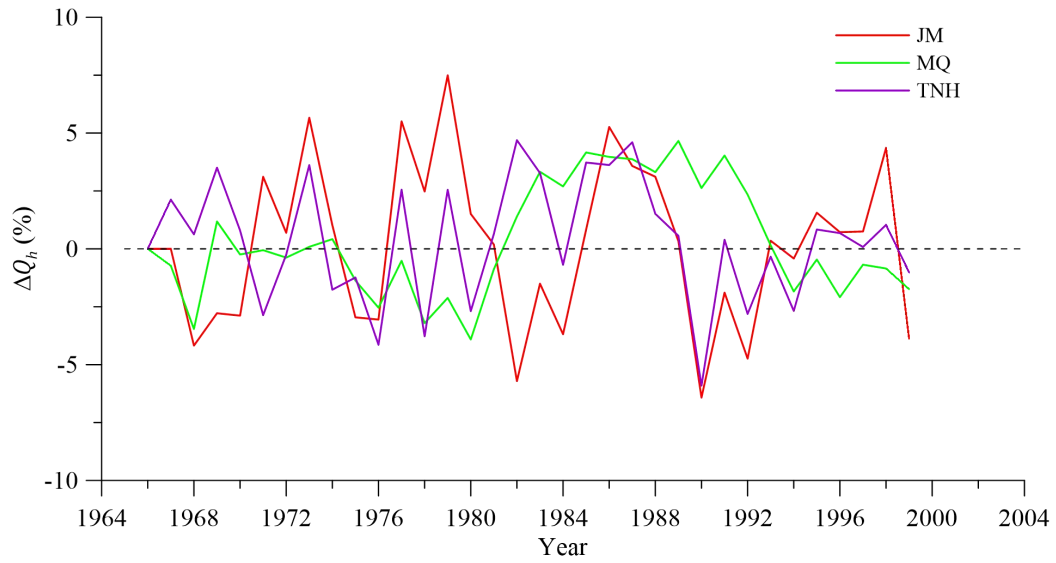
5

Figure 8 Time series of ΔQ_h that obtained by using Eq. (17)

Table 1 Previous study of discharge change of the Yellow River

Main types of study		Data/Method used	Study area	Main causes of discharge change
Data analysis	Yang et al.(2004)	Data from 108 meteorological stations and irrigation data	The Yellow River basin	Decrease in precipitation and increase in evapotranspiration
	Zheng et al. (2007)	Non-parametric Mann–Kendall test and flow duration curve	Sub-basins above Tangnaihai station	Decreasing of wet-season rainfall
	Liang et al. (2010)	Wavelet method	Sub-basins above Huangheyan Station	Climatic variations.
Process based modeling	Tang et al. (2007)	DBD model	The Yellow River basin	In the upper and middle reaches: climate change
	Tang et al. (2013)	SWAT	Sub-basins above Huayuankou station	Precipitation decrease in 1990s
	Cuo et al. (2013)	VIC	Sub-basins above Jingyuan County	Climate change is primary cause for discharge change above Tangnaihai station
	Meng et al. (2016)	VIC	Sub-basins above Tangnaihai station	Changes of precipitation and evapotranspiration
Climate elasticity	Zheng et al. (2009)	Climate elasticity based on Budyko type equations	Sub-basins above Tangnaihai station	Land use change
	Zhao et al. (2009)	Climate elasticity based on Zhang's equation	Sub-basins above Lanzhou station	Climate change and human activity

Table 2 Sub-basins characteristics

	Slop(°)	Area（km²）	Permafrost (%)	Seasonally Frozen Ground (%)
JM	5.86	45308	80%	20%
MQ	11.21	40920	23%	77%
TNH	14.03	36695	46%	54%

Table 3 Proposed formulas of E/P versus E_0/P in the Budyko framework

Types	Solutions	Equations
Non-parametric formulas	Schreiber (Schreiber,1901)	$1-e^{\frac{E_0}{P}}$
	Ol'dekop (Ol'dekop,1911)	$\dfrac{E_0}{P}\tanh\left(\dfrac{P}{E_0}\right)$
	Budyko (Budyko, 1974)	$\left[\dfrac{E_0}{P}\tanh\left(\dfrac{P}{E_0}\right)\left(1-e^{-\frac{E_0}{P}}\right)\right]^{\frac{1}{2}}$
One-parameter formulas	Fu (Fu,1981;Zhang et al., 2004)	$1+\dfrac{E_0}{P}-\left(1+\left(\dfrac{E_0}{P}\right)^{w}\right)^{\frac{1}{w}}$
	Choudhury (Choudhury,1999; Yang et al., 2008)	$\left(1+\left(\dfrac{E_0}{P}\right)^{-n}\right)^{-\frac{1}{n}}$
	Zhang (Zhang et al., 2001)	$\dfrac{1+\alpha\cdot\dfrac{E_0}{P}}{1+\alpha\cdot\dfrac{E_0}{P}+\dfrac{P}{E_0}}$

Table 4 Results of partitioned changes in discharge using existing methods

Sub-basins	Periods	w			ΔQ_c (%)			ΔQ_h (ΔQ_w) (%)			ΔQ (%)
		C*	S*	D*	C	S	D	C	S	D	
JM	1961-1990	2	2.10	2.10			Reference period				
	1991-2002	2	2.33	2.33	-8.10	-7.25	-7.69	-19.62	-20.67	-20.03	-27.72
	2003-2013	2	2.21	2.21	19.57	16.37	18.60	-13.35	-10.05	-12.38	6.22
MQ	1961-1990	2	1.85	1.85			Reference period				
	1991-2002	2	2.01	2.01	-11.04	-11.20	-11.43	-10.85	-10.74	-10.47	-21.89
	2003-2013	2	2.08	2.08	-1.29	-1.35	-1.18	-15.31	-13.52	-15.42	-16.60
TNH	1961-1990	2	1.74	1.74			Reference period				
	1991-2002	2	1.94	1.94	-8.20	-8.89	-9.37	-19.75	-19.25	-18.58	-27.94
	2003-2013	2	1.86	1.86	6.84	7.34	8.38	-11.86	-11.05	-13.40	-5.02

* The C, S and D indicate the climate elasticity method, sensitivity method and decomposition method, respectively.

5

Table 5 Results of w covariate analysis for the period between 1961 and 2013

Sub-basins	Models of Eq. (15) (Candidates $\overline{P}$, $\overline{E_0}$ and $\overline{T}$)	R^2	Models of Eq. (15) (Candidates $\overline{I}$, $\overline{E_0}$ and $\overline{T}$)	R^2
JM	$4.254+0.357\overline{T}-1.715\overline{P}$	0.67	$5.229+0.466\overline{T}-2.582\overline{I}$	0.83
MQ	$-1.743-1.201\overline{P}+4.874\overline{E_0}$	0.85	$-3.778-1.582\overline{I}+7.291\overline{E_0}$	0.88
TNH	$3.814+0.287\overline{T}-2.281\overline{P}$	0.90	$1.982+0.442\overline{T}-3.194\overline{I}+2.591\overline{E_0}$	0.91

10

Table 6 MFD record length and correlation between CMAT and MAT at observation stations

Station	R^2 of MFD- CMAT	R^2 of MFD- MAT	MFD record length (years)
M5	0.65 (–)*	0.49 (–)	1960-2004(45)
M6	0.29 (–)	0.13 (–)	1983-2004(22)
M7	0.34 (–)	0.053 (–)	1980-2004(25)
M8	0.18 (–)	0.41 (–)	1990-2004(13)
M10	0.21 (–)	0.08 (–)	1962-2004(43)
M11	0.01 (–)	0.18 (–)	1991-2004(14)
M12	0.55 (–)	0.46 (–)	1967-1997(31)
M13	0.58 (–)	0.41 (–)	1974-2004(31)
M14	0.47 (–)	0.24 (–)	1966-2004(39)
M16	0.47 (–)	0.38 (–)	1971-1979 1995-2004(28)
M17	0.52 (–)	0.35 (–)	1974-2004(31)

5 *(–) indicates negative correlation